

SINTEF Building and Infrastructure Tore Myrland Jensen

Diffusion tight concrete – Preliminary study

COIN Project report 9 - 2008



SINTEF Building and Infrastructure

Tore Myrland Jensen

Diffusion tight concrete - Preliminary study

COIN P 3 Innovative construction concepts

SP3.3 Hybrid structures

COIN Project report 9 – 2008

COIN Project report no 9

Tore Myrland Jensen

Diffusion tight concrete - Preliminary study

COIN P 3 Innovative construction concepts

SP3.3 Hybrid structures

Keywords:

Materials technology, concrete

ISSN 1891-1978 (online)

ISBN 978-82-536-1075-7 (pdf)

© Copyright SINTEF Building and Infrastructure 2009

The material in this publication is covered by the provisions of the Norwegian Copyright Act. Without any special agreement with SINTEF Building and Infrastructure, any copying and making available of the material is only allowed to the extent that this is permitted by law or allowed through an agreement with Kopinor, the Reproduction Rights Organisation for Norway. Any use contrary to legislation or an agreement may lead to a liability for damages and confiscation, and may be punished by fines or imprisonment.

Address: Forskningsveien 3 B
POBox 124 Blindern
N-0314 OSLO

Tel: +47 22 96 55 55

Fax: +47 22 69 94 38 and 22 96 55 08

www.sintef.no/byggforsk

www.coinweb.no

Cooperation partners / Consortium Concrete Innovation Centre (COIN)

Aker Solutions

Contact: Jan-Diederik Advocaat

Email: jan-diederik.advocaat@akersolutions.com

Tel: +47 67595050

NTNU

Contact: Terje Kanstad

Email: terje.kanstad@ntnu.no

Tel: +47 73594700

Spenncon AS

Contact: Ingrid Dahl Hovland

Email: ingrid.dahl.hovland@spenncon.no

Tel: +47 67573900

Borregaard Ligno Tech

Contact: Kåre Reknes

Email: kare.reknes@borregaard.com

Tel: +47 69118000

Rescon Mapei AS

Contact: Trond Hagerud

Email: trond.hagerud@resconmapei.no

Tel: +47 69972000

Norwegian Public Roads Administration

Contact: Kjersti K. Dunham

Email: kjersti.kvalheim.dunham@vegvesen.no

Tel: +47 22073940

maxit Group AB

Contact: Geir Norden

Email: geir.norden@maxit.no

Tel: +47 22887700

SINTEF Building and Infrastructure

Contact: Tor Arne Hammer

Email: tor.hammer@sintef.no

Tel: +47 73596856

Unicon AS

Contact: Stein Tosterud

Email: stto@unicon.no

Tel: +47 22309035

Norcem AS

Contact: Terje Rønning

Email: terje.ronning@norcem.no

Tel: +47 35572000

Skanska Norge AS

Contact: Sverre Smeplass

Email: sverre.smeplass@skanska.no

Tel: +47 40013660

Veidekke Entreprenør ASA

Contact: Christine Hauck

Email: christine.hauck@veidekke.no

Tel: +47 21055000

Preface

This study has been carried out within COIN - Concrete Innovation Centre - one of presently 14 Centres for Research based Innovation (CRI), which is an initiative by the Research Council of Norway. The main objective for the CRIs is to enhance the capability of the business sector to innovate by focusing on long-term research based on forging close alliances between research-intensive enterprises and prominent research groups.

The vision of COIN is creation of more attractive concrete buildings and constructions. Attractiveness implies aesthetics, functionality, sustainability, energy efficiency, indoor climate, industrialized construction, improved work environment, and cost efficiency during the whole service life. The primary goal is to fulfil this vision by bringing the development a major leap forward by more fundamental understanding of the mechanisms in order to develop advanced materials, efficient construction techniques and new design concepts combined with more environmentally friendly material production.

The corporate partners are leading multinational companies in the cement and building industry and the aim of COIN is to increase their value creation and strengthen their research activities in Norway. Our over-all ambition is to establish COIN as the display window for concrete innovation in Europe.

About 25 researchers from SINTEF (host), the Norwegian University of Science and Technology - NTNU (research partner) and industry partners, 15 - 20 PhD-students, 5 - 10 MSc-students every year and a number of international guest researchers, work on presently 5 projects:

- Advanced cementing materials and admixtures
- Improved construction techniques
- Innovative construction concepts
- Operational service life design
- Energy efficiency and comfort of concrete structures

COIN has presently a budget of NOK 200 mill over 8 years (from 2007), and is financed by the Research Council of Norway (approx. 40 %), industrial partners (approx 45 %) and by SINTEF Building and Infrastructure and NTNU (in all approx 15 %).

For more information, see www.coinweb.no

Tor Arne Hammer
Centre Manager

Tore Myrland Jensen

Summary

A brief literature review has been made with respect to imperviousness of reinforced concrete structures. Both diffusivity and permeability of reinforced concrete related to gas and liquid penetration are covered, without focus on any specific gas or liquid.

This report gives an overview of factors that may affect the tightness, especially related to cracks and low temperatures. The report also summarizes mechanical and thermal properties of reinforced concrete at low temperatures. Properties at low temperatures that somehow may affect the imperviousness of a reinforced concrete structure are implemented, specially related to possible influence on development of cracks.

To achieve a impervious concrete structure, it is assumed that the main challenge is to avoid crack formation. This can be achieved by a combination of proper structural design and materials technology. If the structure is exposed to cryogenic temperatures, special considerations must be taken due to prevent development of cracks. Most likely it will be important to see this project in relation with the material approach in COIN P1 (advanced cementing materials) and COIN P2 (improved construction technology) with respect to tight concrete structures.

The content in this report is a result of a preliminary study finished within limited time and resources. The conclusion (Ch. 6) may be used as a basis for planning of further research. The report must not be considered as a complete state of the art. In further work it is also necessary to make more specific primary objective regarding to function and acceptance criterion.

Table of contents

TABLE OF CONTENTS	5
1 INTRODUCTION.....	6
2 OBJECTIVE.....	9
3 TIGHTNESS OF CONCRETE STRUCTURES	10
3.1 INTRODUCTION	10
3.2 PERMEABILITY.....	10
3.3 GAS AND LIQUID PENETRATION OF REINFORCED CONCRETE - NEW LITERATURE.....	11
3.4 GAS AND LIQUID PENETRATION OF REINFORCED CONCRETE - THE COSMAR PROJECT	17
4 EFFECTS OF LOW TEMPERATURES.....	24
4.1 INTRODUCTION	24
4.2 CONCRETE PROPERTIES AT LOW TEMPERATURES.....	24
4.2.1 <i>Introduction</i>	24
4.2.2 <i>Compressive strength</i>	24
4.2.3 <i>Tensile splitting strength</i>	27
4.2.4 <i>Modulus of elasticity</i>	29
4.2.5 <i>Ultimate strain capacity</i>	29
4.2.6 <i>Influence of temperature variations</i>	32
4.2.7 <i>Fracture energy and the influence of high strain rate</i>	33
4.2.8 <i>Creep</i>	34
4.2.9 <i>The coefficient of thermal expansion at low temperature</i>	34
4.2.10 <i>Thermal conductivity</i>	36
4.3 STEEL PROPERTIES AT LOW TEMPERATURES	37
4.3.1 <i>Introduction</i>	37
4.3.2 <i>Stress-strain curves</i>	37
4.3.3 <i>Fracture toughness</i>	39
4.3.4 <i>The coefficient of thermal expansion at low temperature</i>	40
4.4 CONSTRUCTIONAL ELEMENTS AT LOW TEMPERATURES	41
4.4.1 <i>Moment capacity</i>	41
4.4.2 <i>Shear capacity</i>	43
4.4.3 <i>Bonding – and anchor capacity</i>	45
4.5 CONCLUDING REMARKS DUE TO LOW TEMPERATURES.....	45
4.5.1 <i>Concrete properties at low temperatures</i>	45
4.5.2 <i>Steel properties at low temperature</i>	46
4.5.3 <i>Construction elements at low temperature</i>	46
5 EFFECT OF WATER PRESSURE ON CONCRETE STRUCTURES.....	48
6 CONCLUSIONS AND FURTHER RESEARCH.....	49
REFERENCES	51

1 Introduction

Concrete is known to be a porous material that somehow can get penetrated by gas or liquid due to both diffusion as a result of concentration gradients, and other transport mechanisms like capillary suction as a result of cycles of wetting and drying. Transport mechanism due to possible pressure gradients (e.g. in LNG tanks) must also be implemented when the imperviousness of a concrete structure is evaluated.

It is of great interest to develop concrete structures that work as a tight barrier against intrusion of gas or liquid without the usual application of an external tight membrane.

This report gives an overview of factors that may affect the imperviousness of a concrete structure, especially related to cracks and low temperatures.

In the following, basic theory due to diffusion and permeability is presented in general.

Diffusion

Diffusion (result of concentration gradients) **through** (steady state flow) porous media, e.g. concrete, can be modelled by a linear diffusion equation, Fick's 1st law, in the following form for one dimension;

$$J = -D \cdot \frac{\delta C}{\delta t} \quad (1.1)$$

$$J = -\frac{D_{\text{eff}} \cdot A \cdot \Delta C}{L} \quad (1.2)$$

Where J is the quantity of substance in question diffused per time interval [mol/s or g/s] through the porous media of area A [m²] and thickness L [m], ΔC is the concentration difference of the substance [mol/m³ or g/m³] across the material thickness L and D_{eff} is the effective diffusion coefficient [m²/s]. J is often called the flux of substance diffusing.

Diffusion **into** (non-steady state flow) a porous media like concrete can be modelled by Fick's 2nd law of diffusion for one dimension;

$$\frac{\delta C}{\delta t} = D \cdot \frac{\delta^2 C}{\delta x^2} \quad (1.3)$$

where

- C = molecule concentration
- t = exposure time
- D = diffusion coefficient
- x = distance from exposed surface

Considering a constant diffusion coefficient an analytical solution of Eq. (1.3) has the form

$$C(x,t) = C_s - (C_s - C_i) \cdot \text{erf} \cdot \frac{x}{2\sqrt{D \cdot t}} \quad (1.4)$$

where

- C(x,t) = gas or liquid concentration in the concrete
- C_s = gas or liquid concentration in the environment
- erf = the error function

The diffusion coefficient D , depends among other things on:

- Porosity
- Amount of cracks, crack widths and crack depths
- w/c ratio
- Type of cement
- Degree of hydration
- Content of pozzolanas
- Exposure time, see Eq. (1.5)
- Temperature, see Eq. (1.6)

Note that several of the preceding factors are strongly coupled. For instance will increased **w/c** ratio mean increased **porosity**.

The diffusion coefficient at different exposure time is often found to be well predicted by

$$D_{t_i} = D_{t_0} \cdot (t_0 / t_i)^\alpha \quad (1.5)$$

where

- D_{t_i} = the diffusion coefficient at time t_i
- D_{t_0} = the diffusion coefficient at time t_0
- α = aging parameter between 0 and 1, dependent on concrete and environment

The diffusion coefficient at different temperatures is often found to be well predicted by

$$D_{T_2} = D_{T_1} \cdot e^{\frac{E_A}{R} \left(\frac{1}{T_1} - \frac{1}{T_2} \right)} \quad (1.6)$$

where

- D_{T_1} = the diffusion coefficient at temperature T_1
- D_{T_2} = the diffusion coefficient temperature T_2
- E_A = the activation energy for diffusion [J/mol]
- T = the temperature [K]
- R = the gas constant [J/K·mol]

Many analytical problems arise when Fick's 2nd law is integrated for finite geometries with discontinuities like notches and cracks, which is relevant for concrete.

Permeability

Permeability is the ability of fluids and gases to flow through porous media like concrete under the influence of a constant pressure difference over the specimen.

Darcy's law, se Eq. (1.7), is a simple proportional relationship between the instantaneous discharge rate through a porous medium (also called flux), the viscosity of the fluid and the pressure drop over a given media thickness.

$$Q = \frac{-\kappa \cdot A}{\mu} \cdot \frac{(P_b - P_a)}{L} \quad (1.7)$$

where

- Q = total discharge [m^3/s]
- κ = permeability coefficient [m^2]
- $(P_b - P_a)$ = constant pressure drop [$\text{Pa} = \text{N}/\text{m}^2 = \text{kg}/\text{m}\cdot\text{s}^2$]
- μ = the dynamic viscosity of the fluid [$\text{kg}/\text{m}\cdot\text{s}$]
- L = length the pressure drop is taking place over (e.g. wall thickness) [m]
- A = area of penetrated medium perpendicular to the direction of Q [m^2]

The total discharge, Q [m^3/s], is equal to the product of the permeability coefficient, κ [m^2], of the medium, the cross-sectional area, A [m^2], perpendicular to the flow direction and the pressure drop, $(P_b - P_a)$ [Pa], all divided by the dynamic viscosity, μ [$\text{kg}/\text{m}\cdot\text{s}$ or $\text{Pa}\cdot\text{s}$], and the thickness,

L [m], of the media experiencing the pressure drop.

Darcy's law is a simple mathematical statement which neatly summarizes several familiar properties, including:

- if there is no pressure gradient over a distance, no flow occurs (this is hydrostatic conditions),
- if there is a pressure gradient, flow will occur from high pressure towards low pressure (opposite the direction of increasing gradient - hence the negative sign in Darcy's law),
- the greater the pressure gradient (through the same formation material), the greater the discharge rate, and
- the discharge rate of fluid will often be different — through different formation materials (or even through the same material, in a different direction) — even if the same pressure gradient exists in both cases.

For composite materials such as concrete, modification of Darcy's law is necessary for calculation of permeability.

Cracks in reinforced concrete structures

In concrete, micro cracks already exist due to its condition as a composite material. Some other cracks develop when concrete is exposed to environmental gradients or service loads. Therefore, studies on cracked reinforced concrete are essential.

Both new and older literature have shown that cracks have a significant influence on both diffusivity and permeability of a concrete structure. For example the influence of crack width on the diffusion coefficient, D , of CO_2 is illustrated in Ch 3.3. Similar influence on the permeability coefficient for liquids, κ , is illustrated in Ch. 3.4. A literature review on effects of low temperature is shown in Ch. 4. This is included due to possible direct and indirect influence on development of cracks, together with direct influence on the permeability for the un-cracked material.

2 Objective

The objective of this report is to make a brief review of factors that somehow may affect the imperviousness of a concrete structure. The focus is on tightness of reinforced concrete structures specially related to cracks and possible effects of low temperatures, herein cryogenic conditions.

The content in this report is a result of a preliminary study finished within limited time and resources. The conclusion (Ch. 6) may be used as a basis for planning of further research.

3 Tightness of concrete structures

3.1 Introduction

The imperviousness or tightness, i.e. the inverse of permeability, of concrete is primarily governed by the w/c-ratio (mass ratio) and the degree of hydration. Tightness is also closely related to the pore structure of the concrete, where the connectivity of the pores is very important as well as the tortuosity. The effect of the pore structure in aggregates and cement paste has to be looked upon separately (see COIN P1), but is generally believed that the permeability of normal weight aggregate is less than the cementitious binder at least the first year. However, this is not necessarily true. Tab. 3.1 shows the permeability coefficient for a number of rocks and the corresponding w/c of a fully hydrated cement paste [48].

Table 3.1 Permeability of some rocks compared to that of fully hydrated cement paste [48]

Rock type	Permeability coefficient (10^{-12} m/s)	w/c of fully hydrated cement paste with same permeability
dense igneous rock	0.0247	0.38
quartz-diorite	0.0824	0.42
marble	0.239	0.48
marble	5.77	0.66
granite	53.5	0.70
sandstone	123	0.71
granite	156	0.71

In the following tightness of concrete structures is reviewed. In this relation, possible cracks related to temperature gradient, shear and bending, hydration, etc. are very determining for the imperviousness regarding to both diffusion (concentration gradients) and permeation (pressure gradients).

Cracks become a main path for gas and liquid penetration inside concrete, so that e.g. the diffusion is accelerated in cracked concrete. Cracks that are through a concrete structure are of course very critical for the tightness of the structure.

Permeability (permeability coefficient) and diffusivity (diffusion coefficient) in sound and cracked concrete also depend on the sort of gas or fluid a concrete structure is exposed to.

3.2 Permeability

Low permeability coefficient is an important property for concrete used in e.g. storage tanks. In general the concretes w/c-ratio is the most important parameter. For gas penetration caused by pressure gradients, the degree of water saturation has considerable influence. Experiments with nitrogen gas permeability indicate that the permeability coefficient for humid concrete reduces with cryogenic temperature, but the coefficient changes less than a factor of about 10^{-1} .

Therefore the influence of temperature depression and appurtenant ice formation seem to be essential less than the influence of the concrete composition and water content.

This may be different for fluid penetration, especially if the fluid react with the water and make a tight solid in the concrete at low temperature, which is the case for the system methane/ice.

3.3 Gas and liquid penetration of reinforced concrete - new literature

A simplified research in new literature related to diffusion and permeability of concrete structures has been made, see Tab. 3.2. Only reference [33] from Tab. 3.2 is briefly reviewed in the following. This is more like an approach to the problem related to permeability and diffusivity of concrete structures.

Table 3.2

Simplified literature research related to gas and liquid penetration of concrete structures

Theme	Reference	Short description/headwords
Review	[26]	Review that summarises the availability and utility of experimental data on the rates of spread and vaporisation of spillages of pressure liquefied and cryogenic liquids on a variety of surfaces including concrete.
Permeability and diffusivity of concrete as function of temperature, cracks, degree of saturation, etc.	[27] [28] [29] [30] [31] [32] [33] [34]	Modelling and experiments of gas and liquid transport through concrete structures, herein effects of: - temperature - crack width - degree of saturation - w/c ratio - pore radius - porosity - self-healing of cracks - molecular diffusion - Knudsen diffusion - damage on permeability - etc.
Influence of cracks on chloride diffusion into concrete	[35] [36]	Modelling and experiments of chloride diffusion into concrete, herein effects of: - crack depth - crack width - concrete age - cement content - w/c ratio
Simulation of diffusion of cryogenic gas like LNG	[37]	Simulation of important aspects of the diffusion of a cryogenic gas like LNG by using a numerical model and wind tunnel.

A brief summary of the main results from [27] to [34]:

1. Permeability and diffusivity of concrete as function of temperature:
 - Considerable increase of permeability and diffusivity of concrete with temperature.
 - Considerable variation depending on types of concrete.
 - Reasonable to good agreement between theory and experiment.

2. Permeability and diffusivity of concrete as function of different cracks:
 - Non-structural (limited depth) cracks have less influence on the diffusivity than structural cracks going through the concrete.
 - Both permeability and diffusivity are strongly affected by increasing crack widths and crack depths.
 - Faster healing of cracks that have a smaller crack width.
3. Permeability of concrete as function of degree of water saturation:
 - Gas permeability decreases considerably with increasing degree of water saturation.
 - Liquid (water) permeability increases considerably when degree of water saturation reaches a certain limit.
4. Permeability and diffusivity of concrete as function of w/c ratio and pore radius:
 - Both permeability and diffusivity decrease considerable with decreasing w/c ratio.
 - The flux seems to become independent of pore radius as the average pore radius exceeds a certain limit (about 30 nm), and this limit varies slightly with total porosity.
5. The effect of cracking is relative more determining for tight materials with a low diffusion coefficient for the un-cracked (sound) material.

A brief summary of the main results from [35] and [36]:

1. The chloride diffusion coefficient increases with increasing crack depth.
2. The chloride diffusion coefficient increases with increasing crack width up to a given value, however the relationship is not clear.
3. The diffusion coefficient through the crack seems to be independent of material parameters.

Influence of cracks on the diffusivity of concrete

H. Song at al. [33] developed an analytical technique for carbonation prediction in early-aged cracked concrete for considering both CO₂ diffusion in sound and cracked concrete.

The CO₂ diffusion in cracked concrete can be formulated by averaging the CO₂ diffusion in sound concrete volume, which does not have cracks, and the CO₂ diffusion in cracked concrete volume having different crack widths. Equivalent diffusivity of CO₂ in cracked concrete is derived analytically with an assumption that liquid and gaseous flow rate of CO₂ (mol/s) are constant in the so-called representative element volume (REV) of cracked concrete, see equation (3.1).

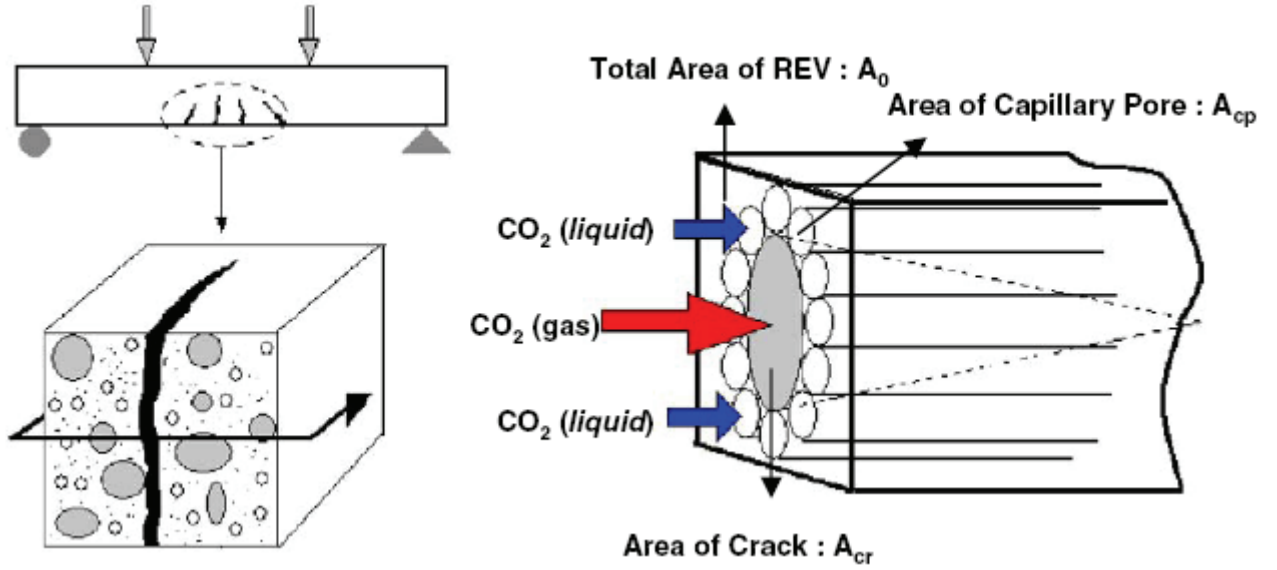


Figure 3.1: Representative element volume (REV) in cracked concrete [33]

Equivalent CO₂ diffusion coefficient (diffusivity) of cracked concrete can be written as

$$D_{CO_2}^{eq} = \frac{\phi(1-S)^4 K_{CO_2}}{\Omega(1+N_K)} D_0^g + \frac{\phi S^4}{\Omega} D_0^d + \frac{K_{CO_2} f(\phi S) \Omega}{R_a \phi S} D_0^g \quad (3.1)$$

where

$D_0^g = 1.0 \cdot 10^{-9} \text{ m}^2/\text{s}$ (basic CO₂ diffusion coefficient for gaseous state)

$D_0^d = 1.34 \cdot 10^{-9} \text{ m}^2/\text{s}$ (basic CO₂ diffusion coefficient for dissolved state)

$R_a = A_0 / A_{cr}$ (total area/crack area)

Ω = average tortuosity of single pore

K_{CO_2} = Equilibrium factor

N_K = Knudsen number

ϕ = Porosity

S = Saturation

$f(\phi S)$ = resistant function representing the characteristics of paths of the cracks

Eq. (3.1) shows that increased crack width, r_{cr} , considered in R_a accelerates diffusion of CO₂ in cracked concrete. First term in Eq. (3.1) represents gaseous CO₂ diffusion in non-saturated pore volume, while second term represents liquid CO₂ diffusion in saturated pore volume. Last term in Eq. (3.1) represents gaseous CO₂ diffusion in crack. CO₂ diffusion in crack is almost the same as CO₂ diffusion in the air. Therefore CO₂ diffusion in crack is expressed with the CO₂ diffusion coefficient in air, D_0^g .

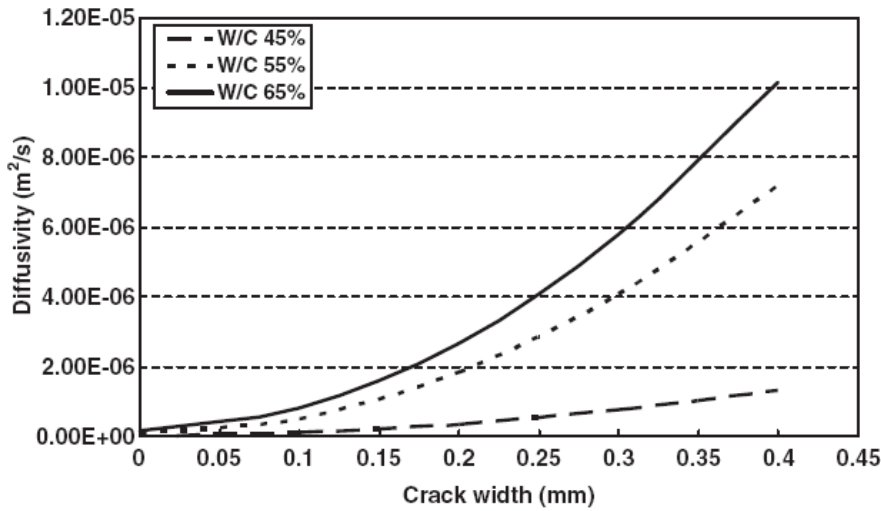


Figure 3.2: Diffusivity of CO_2 vs. crack width for various w/c ratios [33]

The variation of the ratio $D_{CO_2}^{eq} / D_{CO_2}$ (“total diffusivity”/“un-cracked diffusivity”) with the crack width for the different w/c ratios is illustrated in Fig. 3.3.

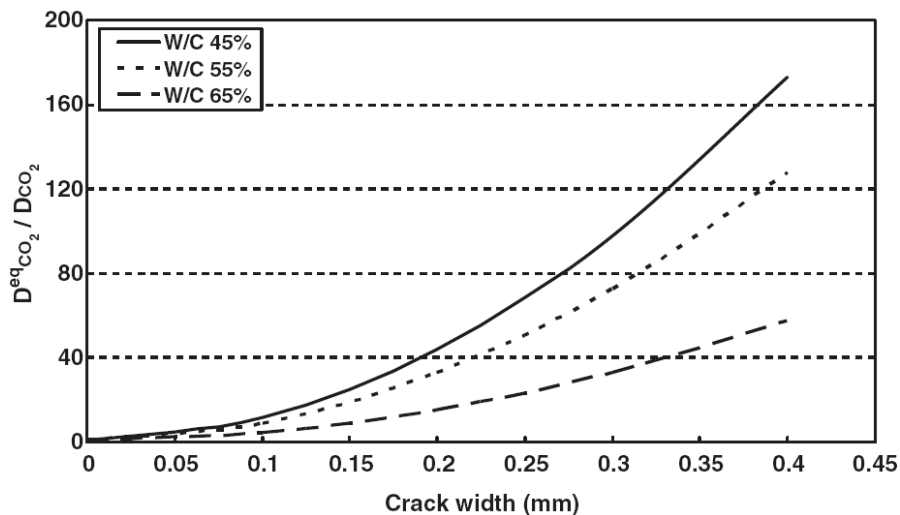
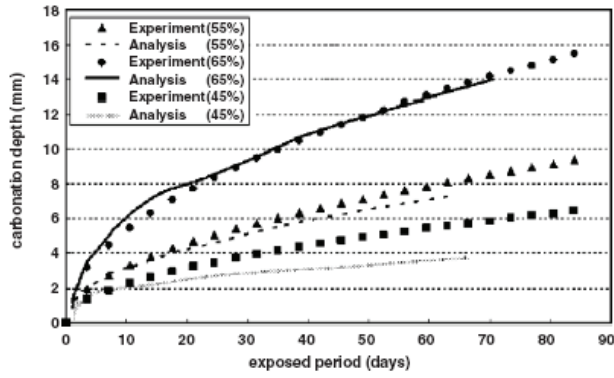


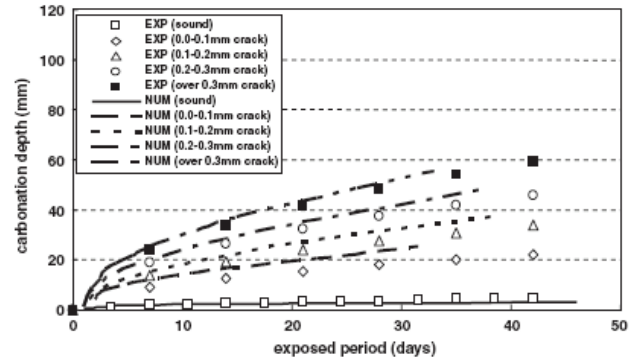
Figure 3.3: Ratio of $D_{CO_2}^{eq} / D_{CO_2}$ vs. crack width for various w/c ratios [33]

The result presented in Fig. 3.3 essentially means that the effect of cracking on $D_{CO_2}^{eq} / D_{CO_2}$ is more important for dense materials with a low diffusion coefficient for the un-cracked material, in this case obtained by lower w/c ratio. This is analogue to the results obtained by A. Djerbi et al. [36], where the effect of cracking on the chloride diffusion is relative more determining for dense materials with a low diffusion coefficient for the un-cracked material.

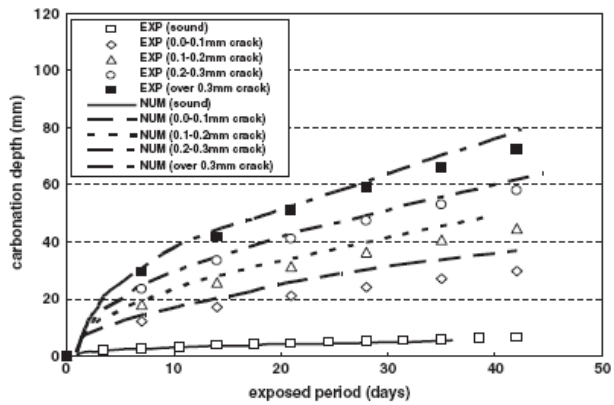
Comparison of experimental data with numerical results obtained gave reasonable results for concrete with three different w/c-ratios (0.45, 0.55 and 0.65) and varying crack widths (see Fig. 3.4).



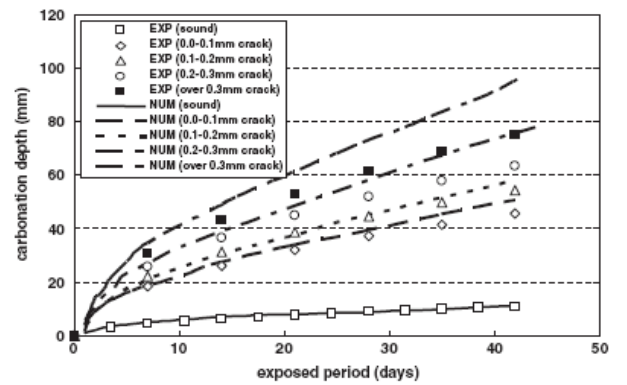
(a) Experimental results in sound concrete



(b) Experimental results in cracked concrete (W/C 45%)



(c) Experimental results in cracked concrete (W/C 55%)



(d) Results in cracked concrete (W/C 65%)

Figure 3.4: Effect of cracks and w/c ratio in carbonation process (diffusion of CO_2) [33]

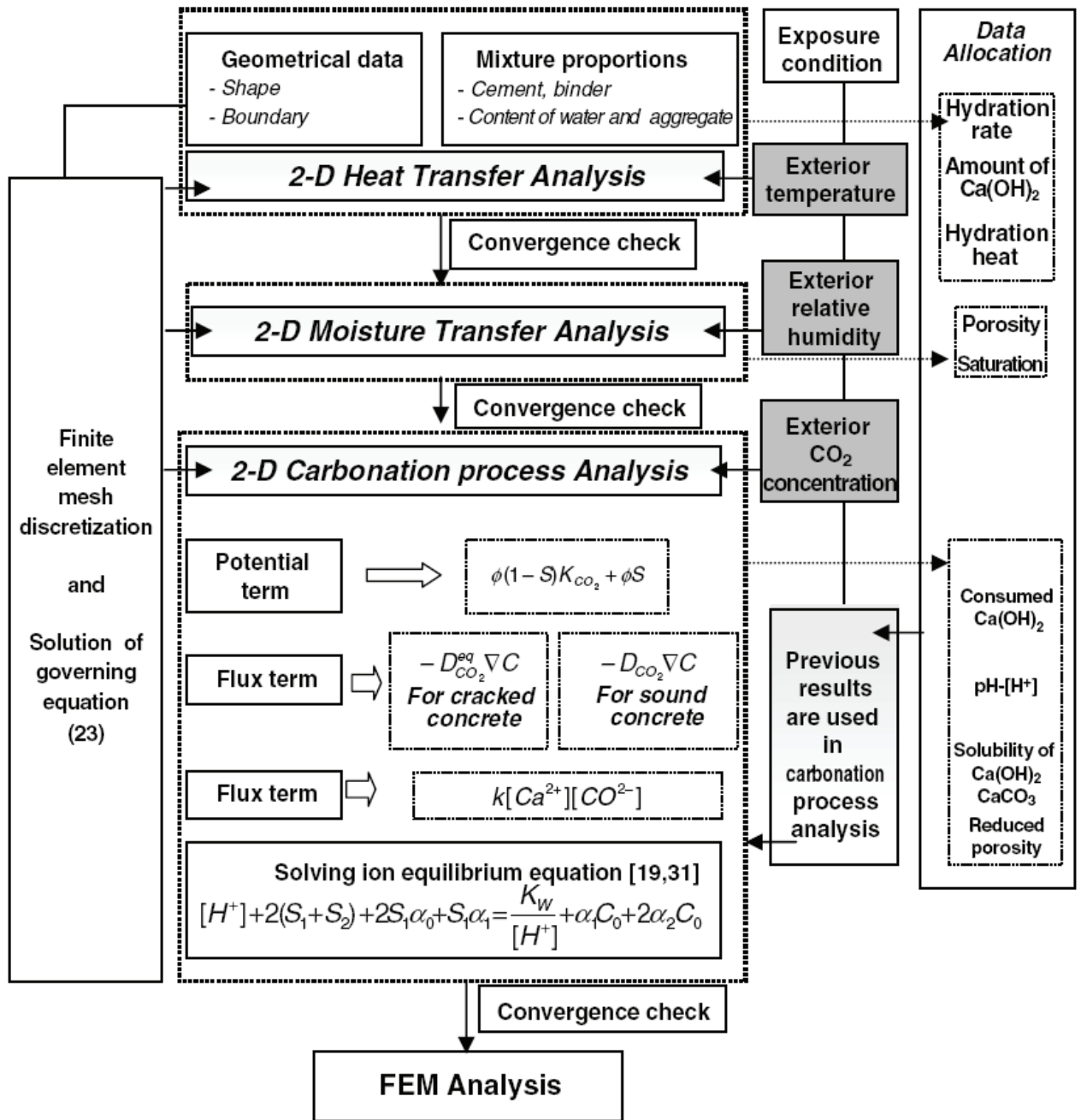


Figure 3.5: Computational scheme of coupled modelling of carbonation in cracked concrete [33]

Fig. 3.5 illustrates the iteration process used for carbonation prediction [33]. The figure also illustrates the complexity of geometrical data, mixture proportions, exposure conditions, etc. that have to be taken into account in the prediction.

Remark:

COIN P4, SP 4.6 STAR: “Residual service life and load bearing capacity of corroded concrete structures”, also review the effect of cracks on the chloride and carbon dioxide penetration of concrete.

3.4 Gas and liquid penetration of reinforced concrete - the COSMAR project

From the project COSMAR sub-project PP3, the following reports are reviewed:

<u>Reference:</u>	<u>Title:</u>
[40]	PP 3-4-4: “Calculation of Leakage Rates of Uncracked and Cracked Concrete structures”
[41]	PP 3-5-3: “Tests for Determination of the Permeability of Uncracked Concrete”
[42]	PP 3-5-4: “Tests for Determination of the Permeability of Cracked Concrete”
[43]	PP 3-6-1: “Design Criteria for Marine Concrete LNG Structures”
[44]	PP 3-6-4: “Liquid Tightness of LNG Storage Tanks”
[45]	PP 3-6-6: “Design criteria for concrete LNG tanks in a marine environment”

The content of the reports listed above is not reviewed in detail in the following, but some extracts from the reports are shown. These extracts are related to test procedures and results. Concrete composition and theory to determinate the characteristic value of permeability are not extracted. The investigation due to permeability worked out in [40] to [45] did not take into account effects related to cryogenic temperatures.

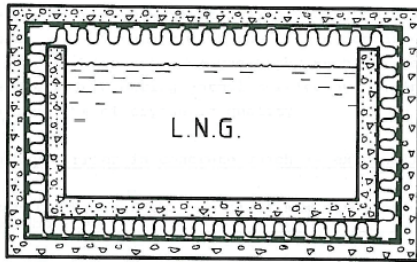
Serviceability limit state of liquid tightness [43]:

For concrete barriers it will be necessary to specify serviceability criteria for tightness. Material specifications must be given providing for concrete of sufficiently low permeability. Similarly details such as construction joints, formwork ties and inserts will have to be treated.

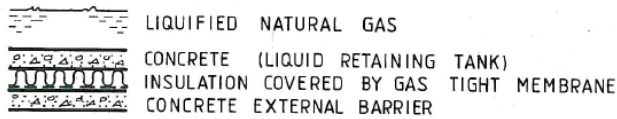
Tab. 3.3 shows the number and types of land storage tanks for LNG up to 1978. The great majority of tanks are seen to be of type 1. Concept for a concrete LNG storage tank type II is shown in Fig. 3.6.

Table 3.3: Statistics of different storage tank types (1978) [45]

Tanktype	: In	: Under	: Planned	: Total
	: Operation	: Construction	: Planned	: Total
Type I	:	:	:	:
Innertank of 9% Ni-steel:	:	:	:	:
or aluminium.	:	:	:	:
Outertank of Carbon steel:	:	:	:	:
Earthdiked impounding area.:	171	15	41	227
Type II	:	:	:	:
Innertank and outertank	:	:	:	:
of concrete.	:	:	:	:
Outertank arranged for	:	:	:	:
containment of leaked LNG.:	4	3	-	7
Type III	:	:	:	:
Innertank of 9% Ni-steel	:	:	:	:
or aluminium.Outertank	:	:	:	:
of concrete arranged for	:	:	:	:
containment of leaked LNG .:	1	1	-	2
Type IV	:	:	:	:
Inground storage tanks.	:	:	:	16



DIAGRAMATIC SECTION THROUGH CONCRETE
L.N.G. TANK



DIAGRAMATIC SECTION THROUGH WALL OF
ALL CONCRETE L.N.G. TANK

Figure 3.6: Concept for a concrete LNG storage tank (tank type II) [44]

Tests for determination of the permeability of cracked concrete, [42]:

Fig. 3.7 to 3.9 show the principle of the test arrangement used for determination of permeability of concrete, while Fig. 3.10, 3.11 and Tab. 3.4 show some of the result obtained, due to respectively uncracked and cracked concrete [41], [42].

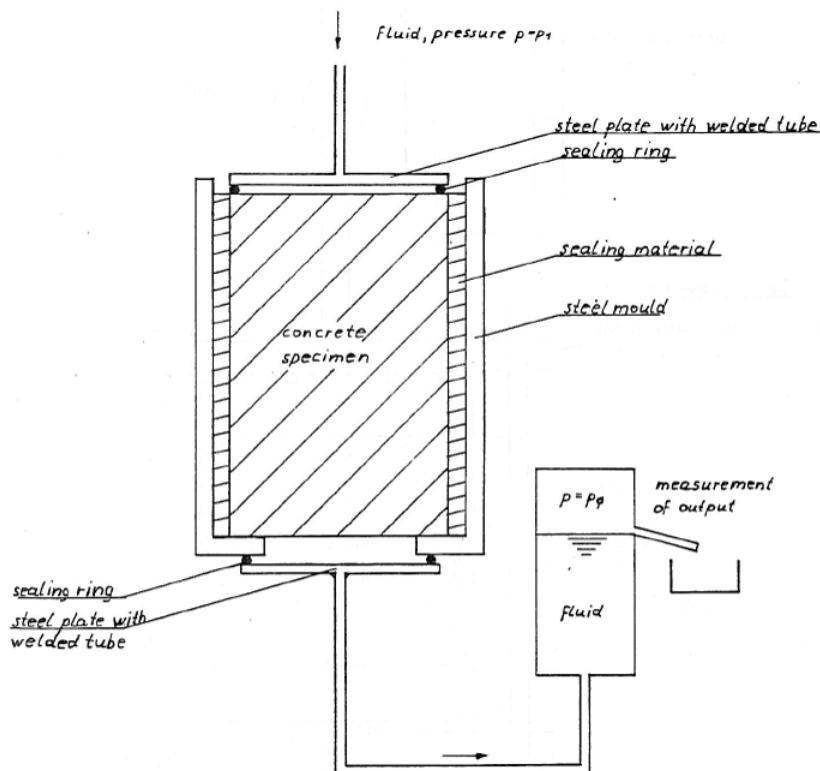


Figure 3.7: Test arrangement principle for determination of fluid-permeability of concrete [40]

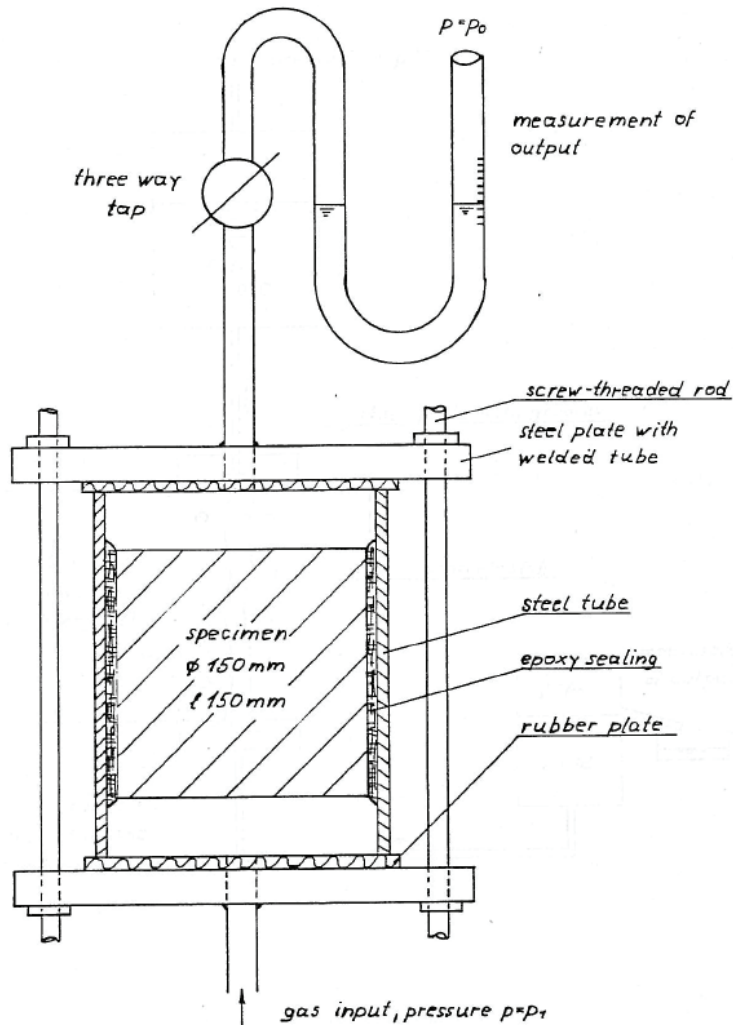


Figure 3.8: Test arrangement principle for determination of gas-permeability of concrete [40]

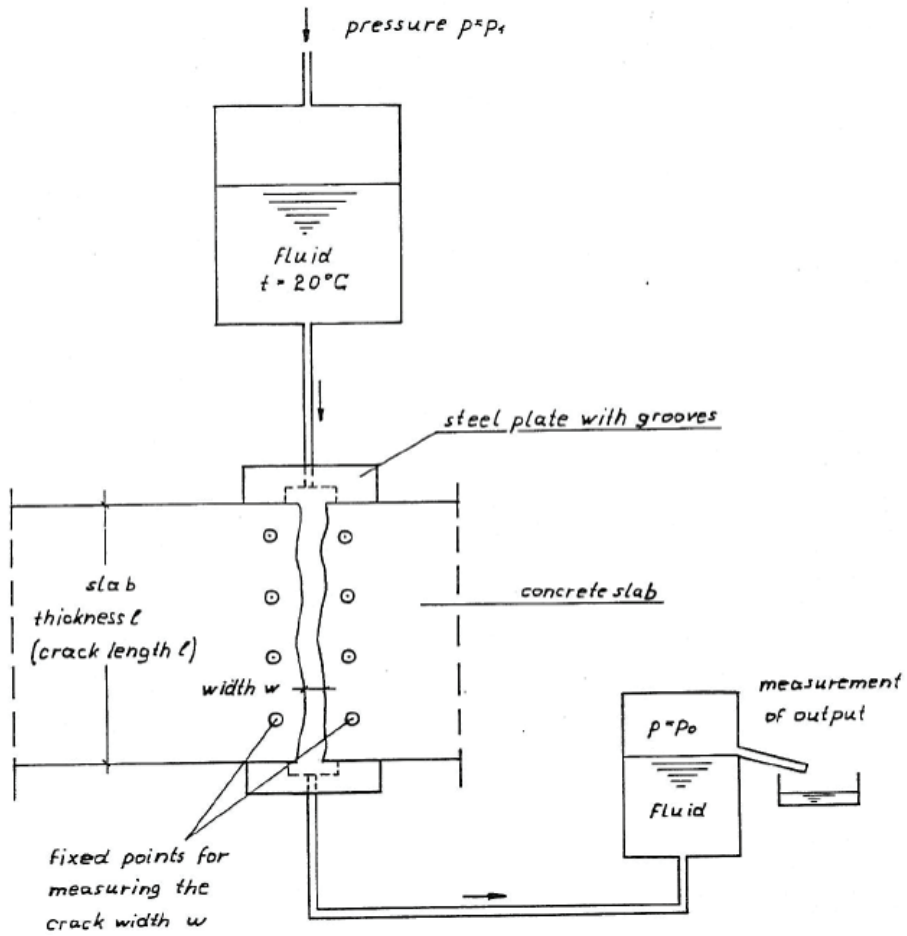


Figure 3.9: Test arrangement principle for determination of permeability of cracks in concrete [40]

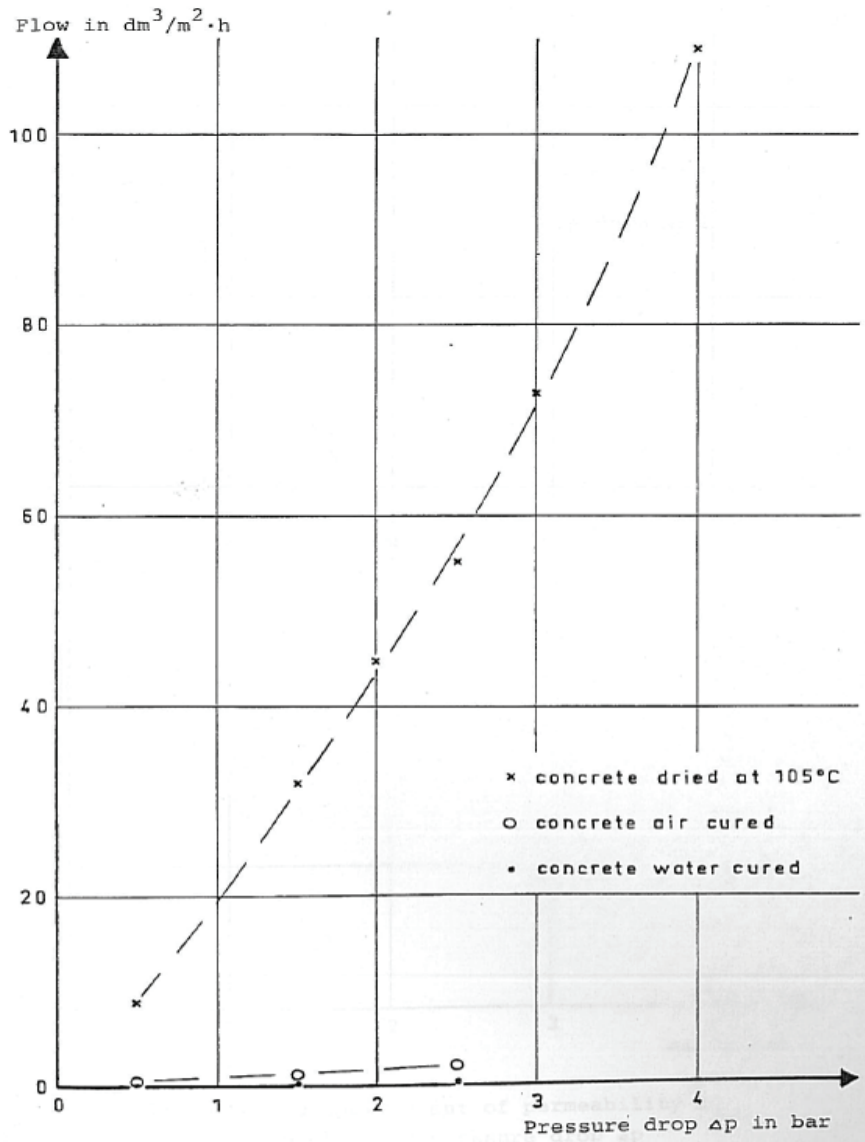


Figure 3.10: Flow of nitrogen as a function of different pressure drops ΔP through 0.15 m thick uncracked concrete at 20°C [41]

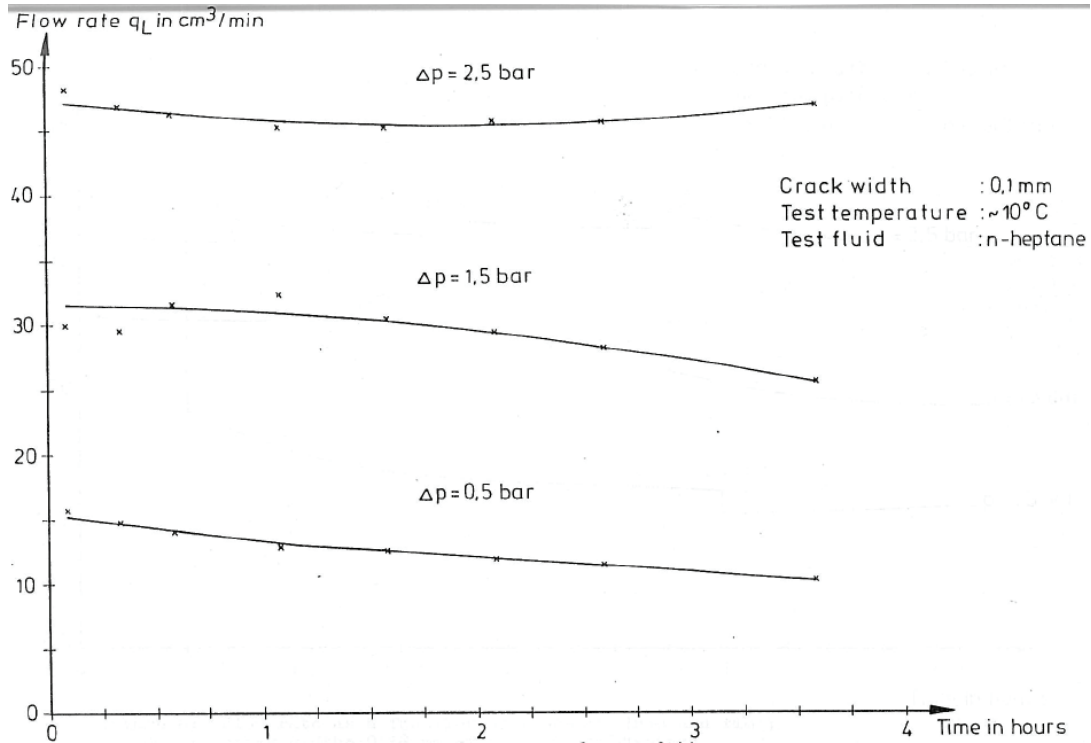


Figure 3.11: Flow rate as a function of pressure drop and time; crack width: 0.10 mm, test fluid: n-heptane [42]

Table 3.4: Flow rate q_L , measured and calculated, as a function of crack width and pressure drop [42]

Crack width w in mm	Pressure drop Δp in bar	Flow rate q_L in cm^3/min of				methane $\nu_{-165^\circ\text{C}} = 0,33 \cdot 10^{-6} \text{ m}^2/\text{s}$ calculated ²⁾
		n-heptane $\nu_{10^\circ\text{C}} = 0,65 \cdot 10^{-6} \text{ m}^2/\text{s}$		water $\nu_{10^\circ\text{C}} = 1,3 \cdot 10^{-6} \text{ m}^2/\text{s}$		
		measured ¹⁾	calculated ²⁾	measured ¹⁾	calculated ²⁾	
0,1	0,5	15,6	19,6		6,63	61,7
	1,5	32,3	58,6	-	19,9	185
	2,5	48,2	97,6		33,2	307
0,18	0,5	371	115		38,7	360
	1,5	255	342	-	116	1080
	2,5	327	570		193	1790
0,28	0,5	577	431	104	146	1350
	1,5	727	1290	198	437	4050
	2,5	938	2140	310	728	6750

1) Measured maximum flow rate

2) Flow rate calculated with relationship $\lambda \times \text{Re} = 3 \times 10^3$

(Crack length: 182 mm, crack breadth: 200 mm)

A brief summary of the main results from [41] and [42]:

1. Considerable influence of varying moisture levels on the gas permeability, see Fig 3.10.
2. Considerable influence of crack widths on the permeability for liquids, see Tab. 3.4.
3. Dependence on pressure drops due to both flow rates of gas and liquids, see Fig. 3.10 and Tab. 3.4.
4. Some time-related reduction in flow rate for cracked concrete, see Fig. 3.11.

Recommendation for design from [44] and [45]:

Under normal service conditions it should at all times be ensured that the concentration of flammable gas in interbarrier voids shall not exceed 30% of the lower flammability level of the relevant gas. Gas detection instrumentation shall be installed to ensure that critical gas concentration does not arise. Interbarrier spaces shall be filled with inert gas.

In the accidental event of primary barrier failure in which the secondary barrier is exposed to liquid natural gas, permeation should be limited to a level ensuring that flammable gas concentration do not exceed 30% of the lower flammability level externally to the secondary barrier. Provided the secondary barrier is externally exposed, the dilution effect provided by natural convection arising adjacent to a cold surface may be taken into account. Membranes incorporated in secondary barrier construction may be taken into account if of cryogenic quality.

Secondary barriers constructed in reinforced or prestressed concrete may be taken to satisfy the above requirement if the following criteria can be satisfied by the following calculations in the accident limit state:

1. The depth of the compressive zone shall at all points exceed 40% of the overall construction depth. If there is a minimum prestress of 0.5 MPa in the external “fibre” on the pressure zone of the concrete, it can be taken that penetrating cracks will not occur.
2. Calculations of gas permeability allowing for crack depth and assuming no resistance to flow in cracks should demonstrate that permeation will not exceed the levels given in the following table:

LNG pool depth	3 m	3 m	10 m
Temperature difference between tank wall surface and ambient	20°C	40°C	40°C
Permissible permeation	0.5 m ³ /m ² h	0.7 m ³ /m ² h	0.4 m ³ /m ² h

3. In the event of a local cool down due to leakage or insulation failure it will be sufficient to document that there will be a residual prestress strain in the extreme “fibre” of the concrete under the assumption of rigid restraint by the surrounding structure

Tightness [45]:

A primary barrier with a concrete structure may or may not be supplemented with an inert gas or inert gas and liquid tight membrane. Concrete may thus be required to act as fluid and gas tight. A concrete barrier can be considered fluid tight providing the fluid permeation will not exceed the rate of boil off in any local area.

4 Effects of low temperatures

4.1 Introduction

In connection with imperviousness of concrete structures it is relevant to look into possible effects of low temperatures. Concrete is known to maintain its favourable properties within a very broad temperature range. However, if a concrete structure is assumed to be exposed to, for instance, liquefied natural gas (LNG) without any inside steel membrane or similar, it is important to understand the effect of low temperature. Low temperatures and cyclic temperature load may have a considerable influence for a reinforced concrete structure regarding tightness with respect to both concentration and pressure gradients.

The following chapters summarize mechanical and thermal properties of reinforced concrete from the literature reviewed. Only properties that may affect the tightness of a reinforced concrete structure due to low temperatures are implemented. Concrete handbooks are also consulted to include any new information.

4.2 Concrete properties at low temperatures

4.2.1 Introduction

Concrete is frequently used, for instance, in storage tanks of liquefied natural gas (LNG) with a boiling point of -162°C . Concrete structures can withstand long duration of high temperatures up to about $+500^{\circ}\text{C}$ and for shorter periods even higher temperatures up to about $1,000-1,200^{\circ}\text{C}$.

Nevertheless, the material response knowledge is still rather limited in particular in view of the serious consequences of material collapse in the actual fields of application.

In this chapter a survey of the concrete properties under low temperatures is given. The behaviour of concrete at low temperatures depends on cement type, w/c-ratio, aggregate, etc. The factor that gives the largest effect is the degree of water saturation. Mechanical properties at low temperature (i.e. below the freezing point of pore water) increase with increasing water saturation.

4.2.2 Compressive strength

Wischers and Dahms [1] have investigated the influence of low temperatures on the compressive strength of a concrete based on Portland cement (w/c = 0.46) and quartz aggregates. They found, as shown in Fig. 4.1, a significant influence of the moisture content. The water cured specimens obtained a compressive strength at -100°C that was three times higher than at $+20^{\circ}\text{C}$. Specimens stored at 50% RH obtained a 50% increase, while specimens dried at $+105^{\circ}\text{C}$ before testing gained an increase of 20% only.

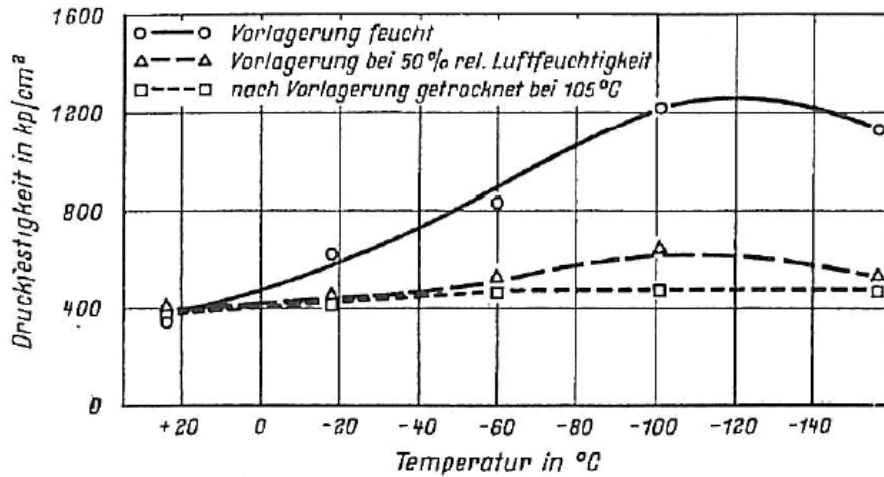


Figure 4.1: The influence of temperature and moisture content on the compressive strength of concrete [1]

The increase of compressive strength at low temperature is, as shown in Fig. 4.2, not as considerable for light weight concrete as for normal weight concrete.

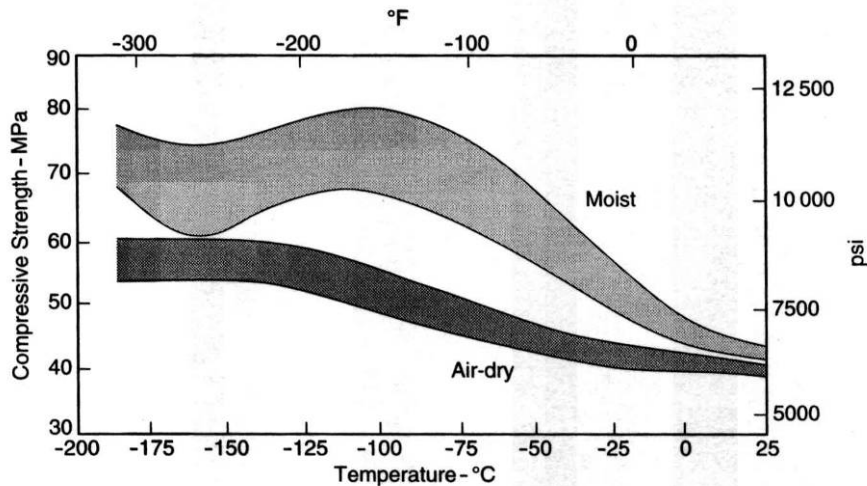


Figure 4.2: The influence of temperature and moisture content on the cylinder strength of light weight concrete [2]

Increase in compressive strength at low temperatures is a result of transformation of liquid water to solid ice. Freezing causes an increase in 10vol% of the “water phase”. Fig. 4.1 and 4.2 indicate that there is little or no increase of the compressive strength below -120°C. The reason is that there is a phase change of ice at -113°C, which cause a volume reduction of 20%.

The increase in compressive strength at -160°C relative to +20°C with increased humidity is independent of w/c-ratio, as shown in Fig. 4.3 [3], because the increase is a result of transformation of liquid water to solid ice.

Rosásy and Wiedeman [5] investigated compressive strength versus low temperature for a 224 days old concrete with w/c = 0.56. Fig. 4.4 gives the relative increase in compressive strength as the temperature decreases.

Compressive strength versus low temperature is also investigated of Marshall [6] versus moisture (Fig. 4.5) and w/c-ratio (Fig. 4.6) and Yamane et al. [7] versus w/c ratio (Fig. 4.7).

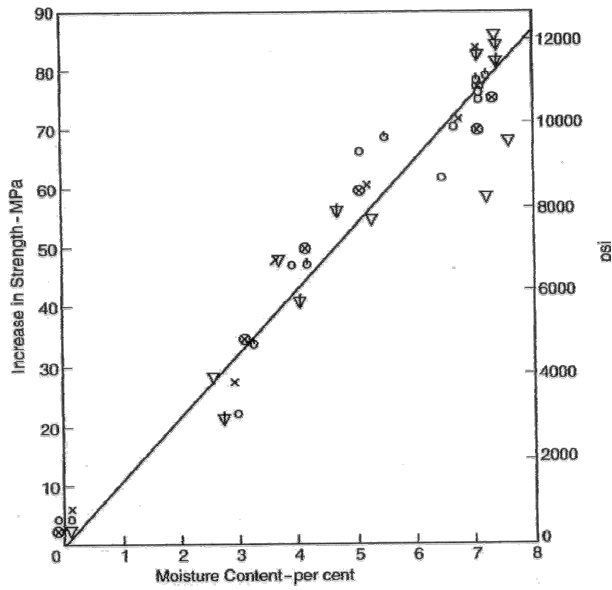


Figure 4.3: Variation of compressive strength versus temperature from +20°C to -160°C and moisture content of concrete with different w/c-ratio [3]

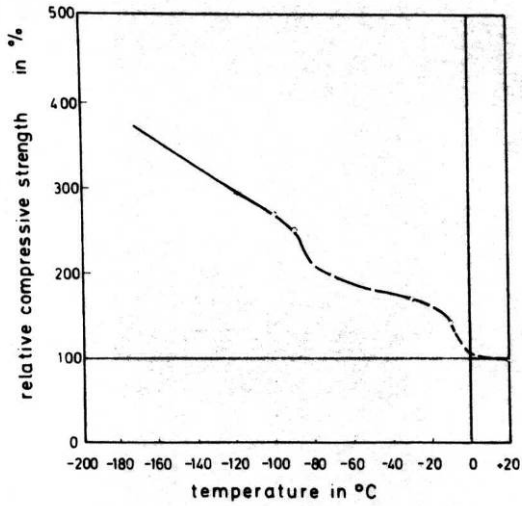


Figure 4.4: Relative compressive strengths (relative to +20°C) versus temperature in water saturated concrete [5]

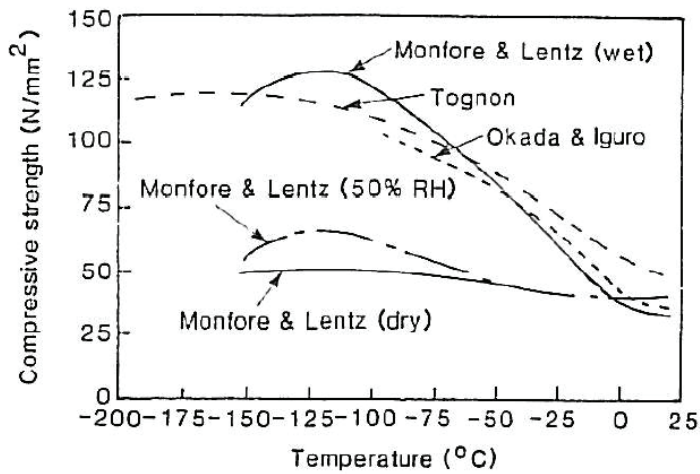


Figure 4.5: Variation of compressive strength with temperature and degree of water saturation [6]

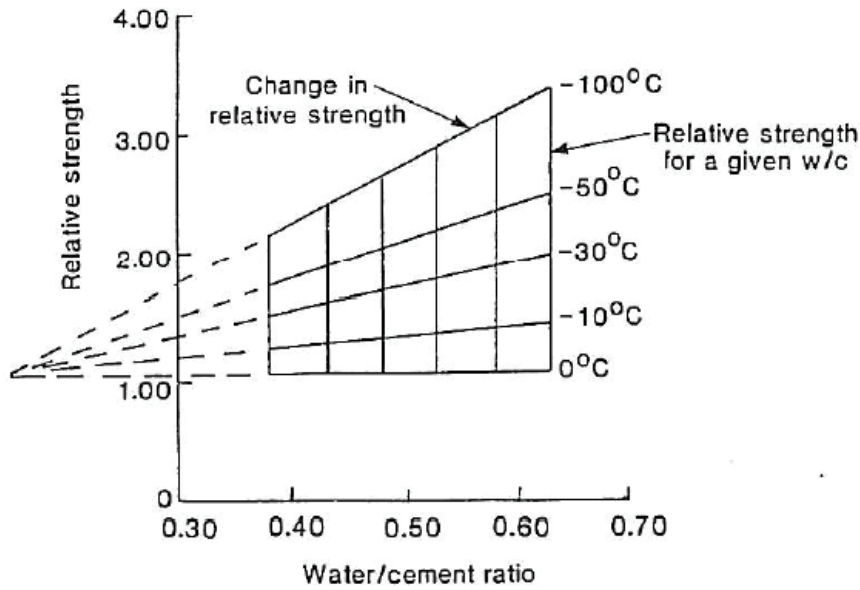


Figure 4.6: Idealized variation in relative strength with w/c-ratio and temperature [6]

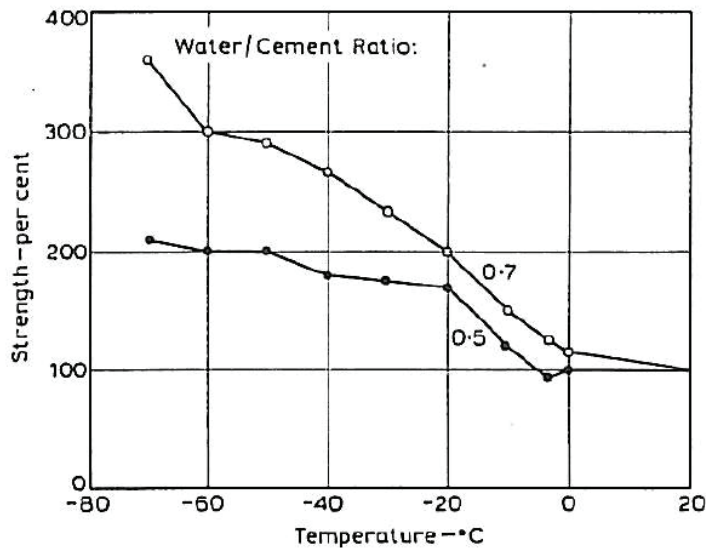


Figure 4.7: Compressive strength of saturated concrete versus temperature and w/c-ratio [7]

4.2.3 Tensile splitting strength

Wischers and Dahms [1] investigated the influence of temperature on the tensile splitting strength. Again, as shown in Fig. 4.8, a significant impact of moisture content is present. The tensile splitting strength shows a more rapid increase with reduced temperature as compared with the compressive strength, while at -100°C the increase in tensile splitting strength is less than in compression. Quite similar response was determined by Turner [8] in test of air-entrained (7 vol %) concrete with w/c ratio 0.43 as shown in Fig. 4.10.

The influence of temperature and moisture content on the tensile splitting strength of light weight concrete, [2], is shown in Fig. 4.9.

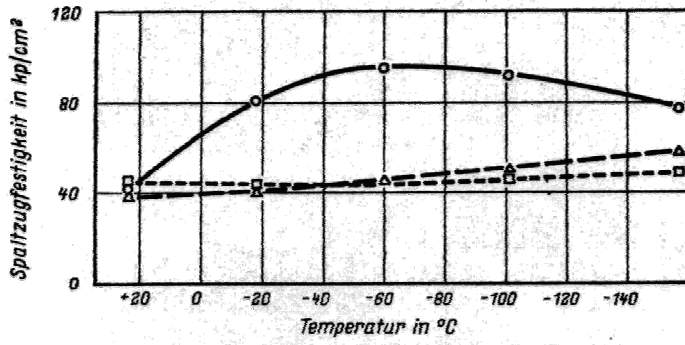


Figure 4.8: The influence of temperature and moisture content on the tensile splitting strength of concrete [1]

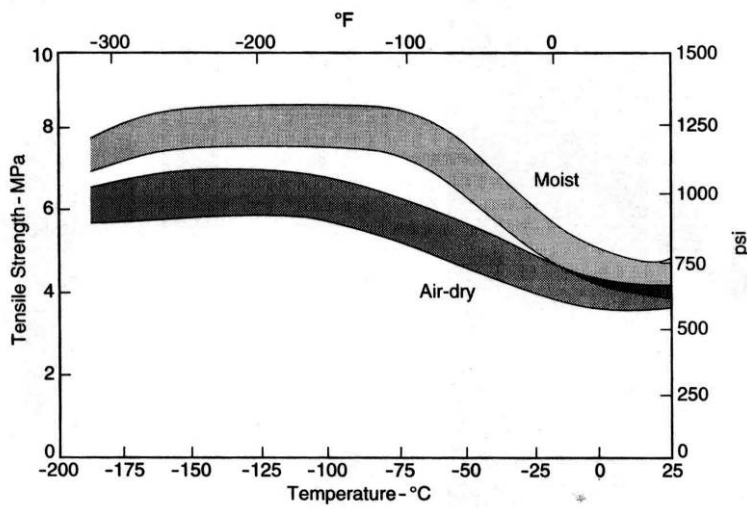


Figure 4.9: The influence of temperature and moisture content on the tensile splitting strength of light weight concrete [2]

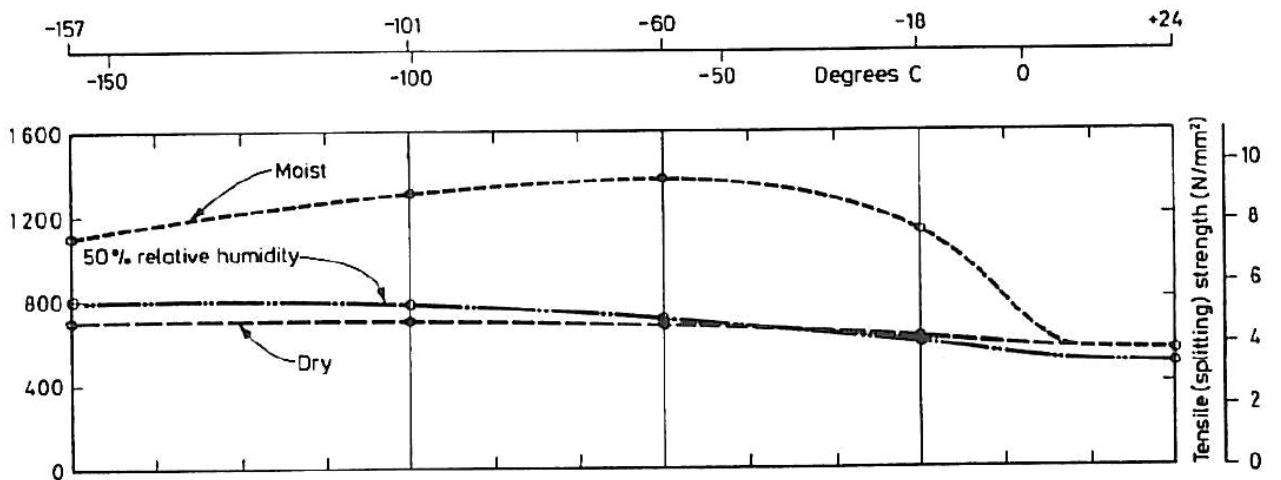


Figure 4.10: Variation in tensile splitting strength with moisture content [8]

4.2.4 Modulus of elasticity

Wischers and Dahms [1] studied the influence of temperature on the modulus of elasticity. The results, Fig. 4.11, show the same influence of moisture content as for the compressive and tensile strengths (Fig. 4.1 and 4.8). The increase due to reduced temperature is, however, less significant and for the moist cured (50% RH) and the dried specimens the increase is negligible.

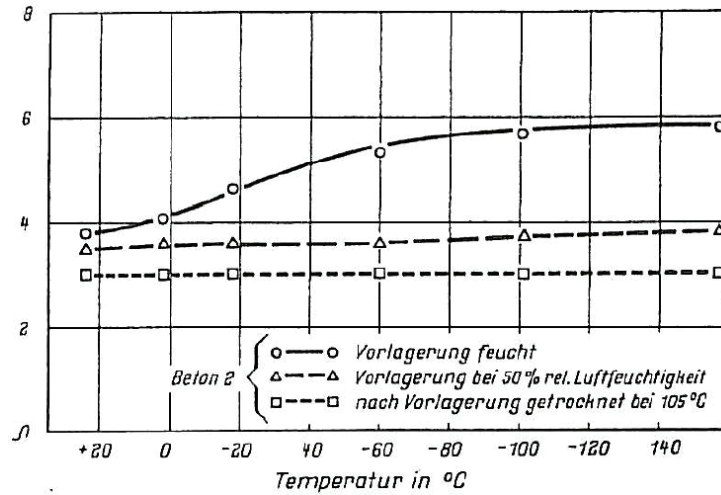


Figure 4.11: The influence of temperature and moisture content on the modulus of elasticity of concrete [1]

4.2.5 Ultimate strain capacity

The results presented in Fig 4.1 and 4.11 indicate that the ultimate strain ought to increase with reduced temperature. Nevertheless, this does not seem to be an unique relation in compression.

Rostásy and Wiedemann [5] determined the compressive stress-strain curves for water saturated concrete at temperatures ranging from +20°C down to -170°C. The curves presented in Fig. 4.12 indicate that the ultimate strain increase down to -70°C, and at further reduction in temperature the strain decrease towards a value less than at +20°C. The reason for this variation in ultimate strain is probably a gradual phase change in the pore structure. However, the author did not have an adequate explanation for the phenomenon.

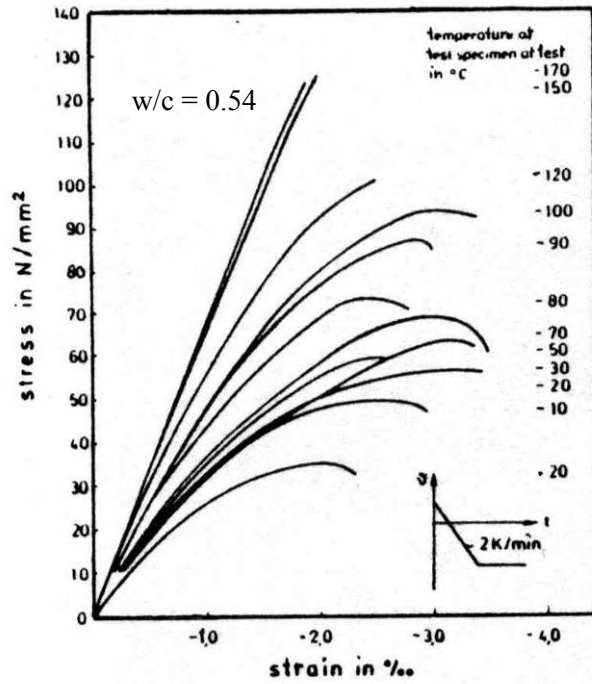


Figure 4.12: Stress- strain curves for water saturated concrete at various temperatures [5]

The relative changes in the ultimate strain from Fig. 4.12 is presented in Fig. 4.13

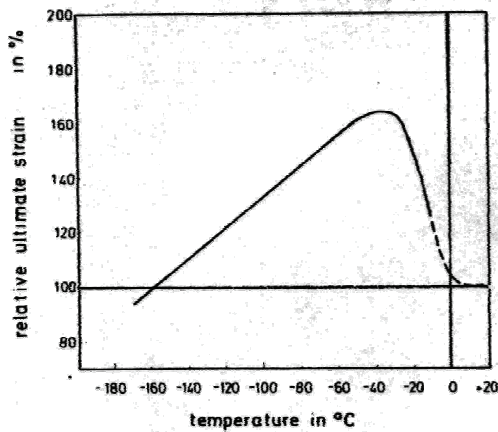


Figure 4.13: Relative compressive strains versus temperature in water saturated concrete [5]

In concrete stored at 65% RH a small increase in strain at $-170^{\circ}C$ is found compared with strain at $+20^{\circ}C$, Fig. 4.14.

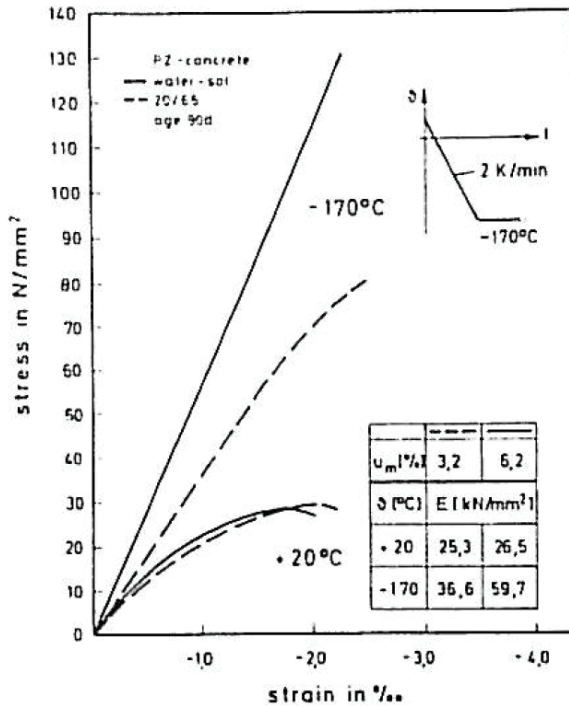


Figure 4.14: Stress- strain curves for concrete with different moisture at +20°C and -170°C [5]

Tests by Hoff [9] on 216 days old concrete stored at 50% RH show that the ultimate strain increases down to -100°C, as shown in Fig. 4.15. Fig. 4.15 does not show the same tendency as Fig. 4.12. This indicates that it is the influence of the water and ice that cause the effects observed in Fig. 4.12.

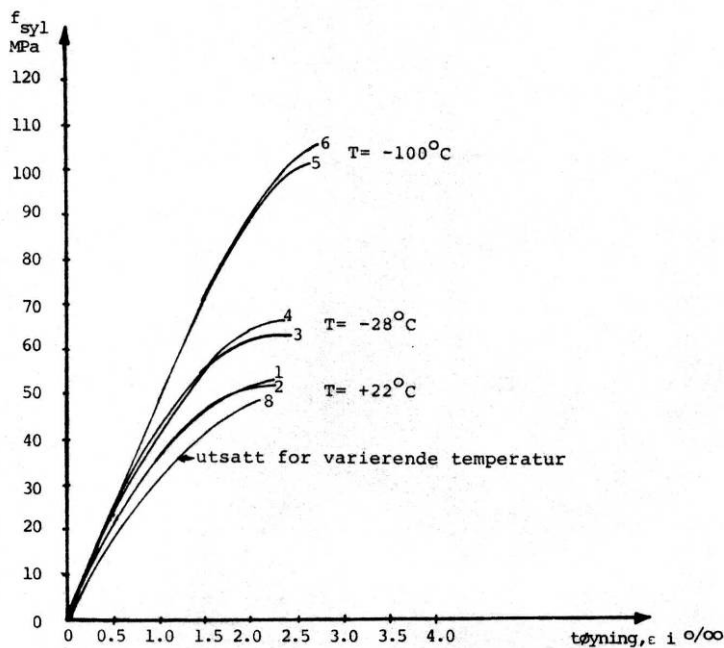


Figure 4.15: Stress- strain curves for concrete stored at 50 % RH [9]

4.2.6 Influence of temperature variations

Freeze-thaw cycles are known to have a deteriorating effect on concrete, if not the concrete has a uniform dispersion of small air bubbles that may unload the pressure from the volume expansion of water turning to ice. It is, therefore, reasonable to assume that temperature variations between ambient and cryogenic temperatures are unfavourable with respect to concrete strength. Such temperature cycles are relevant for storage tanks for LNG. Usually the temperature in storage tanks are reduced according to a strictly defined procedure and then kept at the operating temperature. However, the tank may have to be emptied and, thus, warmed to ambient temperature in cases of technical difficulties like repair of technical installations.

Tests by Rostásy and Wiedeman [10], presented in Fig. 4.16, confirm this assumption. The stress-strain curves determined after various numbers of cycles from +20°C to -170°C and back to +20°C show a considerable reduction in concrete strength and modulus of elasticity after a few cycles. These tests were conducted on water saturated 150 days old mortar with a w/c ratio of 0.5 and a compressive cylinder strength of 49 MPa at 20°C

One cycle +20°C → -170 °C → +20 °C appear, according to Fig. 4.16, to be much more destructive to the concrete than several cycles +20°C → -20°C → +20°C according to ordinary testing of frost resistance.

Even for relative dry concrete samples stored at 50 % relative humidity the experience show considerable reduction in strength and modulus of elasticity for one cycle +22 °C → -28 °C → +22 °C → -100 °C → +22 °C as shown under “cycle” in Tab. 4.1.

Table 4.1: Relative property data for concrete stored at 50 % relative humidity when exposed to different temperatures [9]

Temperature	+22 °C	-28 °C	-100 °C	“cycle”
Fracture stress	1,0	1,23	1,97	0,95
Ultimate strain	1,0	1,08	1,20	0,93
Modulus of elasticity	1,0	1,13	1,20	0,84

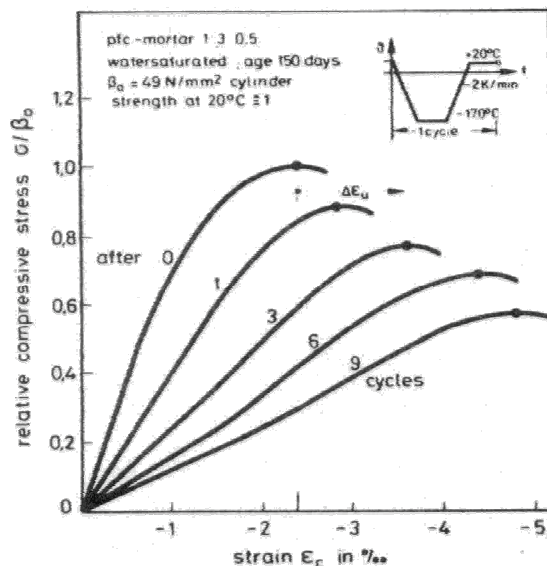


Figure 4.16: Stress- strain curves of mortar specimens subjected to various numbers of temperature cycles (+20°C → -170°C → +20°C) [10]

4.2.7 Fracture energy and the influence of high strain rate

Körmeling [11] investigated the tensile strength and the fracture energy over a wide range of deformation rates, both at +20°C and -170°C. In each case uniaxially tensiled specimens were used. As can be seen from the results in Tab. 4.2 and the load-deformation curves in Fig. 4.17, the tensile strength and the fracture energy has the highest value at -170°C when a low deformation rate is used. When a high deformation rate is applied, the tensile strength at -170°C is smaller than the strength at +20°C. On the other hand the increase in fracture energy at a high deformation rate is almost the same at -170°C and at +20°C.

Table 4.2:

Results from uniaxial tensile test at low and high deformation rates at both +20°C and -170°C [11]

Temperature (°C)	Deformation rate (mm/s)		f_{ct} (N/mm ²)	Δ_{ct} (mm)	G_F (N/m)
+20	Low	$0.125 \cdot 10^{-3}$	3.28 ± 0.44	$0.0123 \pm 0,0021$	131 ± 34
	Intermediate	28	4.79 ± 0.61	$0.0170 \pm 0,0010$	172 ± 18
	High	2400	5.48 ± 0.46	$0.0169 \pm 0,0024$	323 ± 58
-170	Low	$0.125 \cdot 10^{-3}$	4.28 ± 0.14	$0.0142 \pm 0,0008$	205 ± 5
	High	2400	4.99 ± 0.31	$0.0170 \pm 0,0010$	480 ± 66

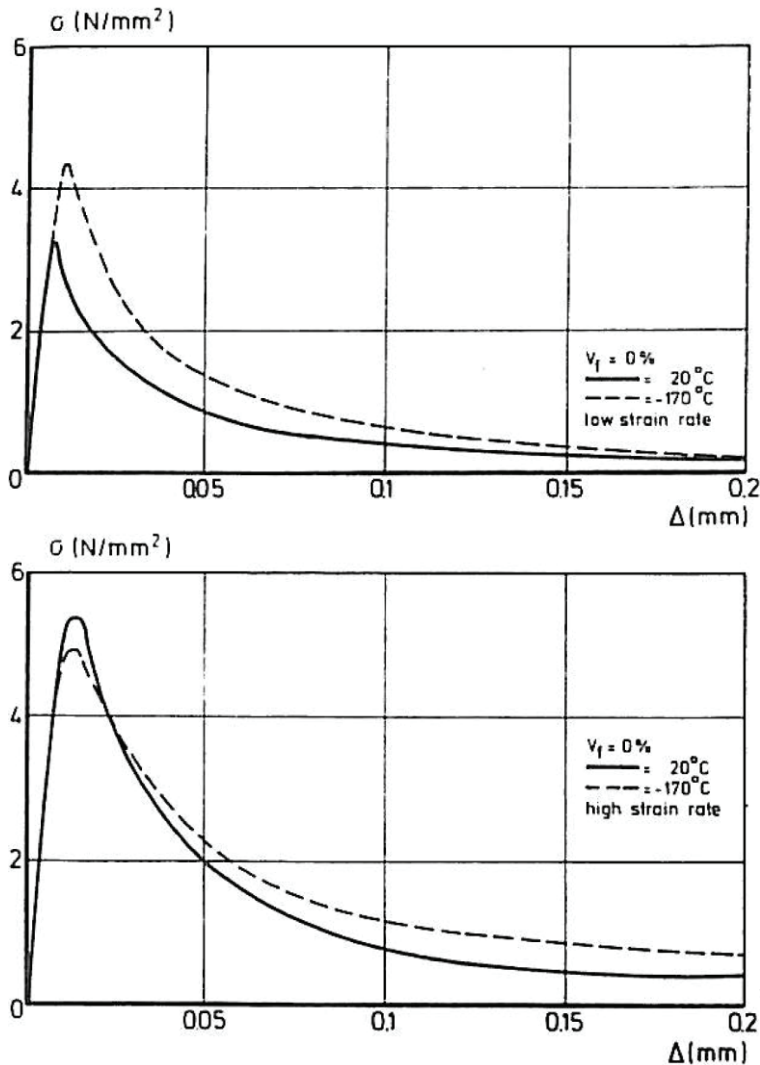


Fig. 4.17: Load-deformation curves for uniaxially tensiled specimens at +20°C and -170°C for both low and high deformation rates [11]

4.2.8 Creep

There are few available results on the influence of low temperature on the creep deformation of concrete. Results from Japan by Okada and Iguro [12] indicate that the creep deformation after 3 months at -30°C is only 50 % of the creep deformation at $+20^{\circ}\text{C}$. There is no good explanation for this phenomenon, but this may be the result of different dehydration.

4.2.9 The coefficient of thermal expansion at low temperature

The influence of temperature on the thermal expansion depends on the concrete moisture content. Tests by Rostásy et al. [13] on water saturated mortar with w/c-ratio 0.8 and 0.5, and on dried mortar with w/c ratio 0.5, presented in Fig. 4.18 (a), clearly reflects this moisture dependency. For the two water saturated mortars an expansion is observed when the temperature is reduced from 0°C to -70°C , while no such expansion is present in the dried specimen. The expansion is related to the freezing of water in the capillary and gel pores, which is reflected in the larger expansion of the most porous mortar.

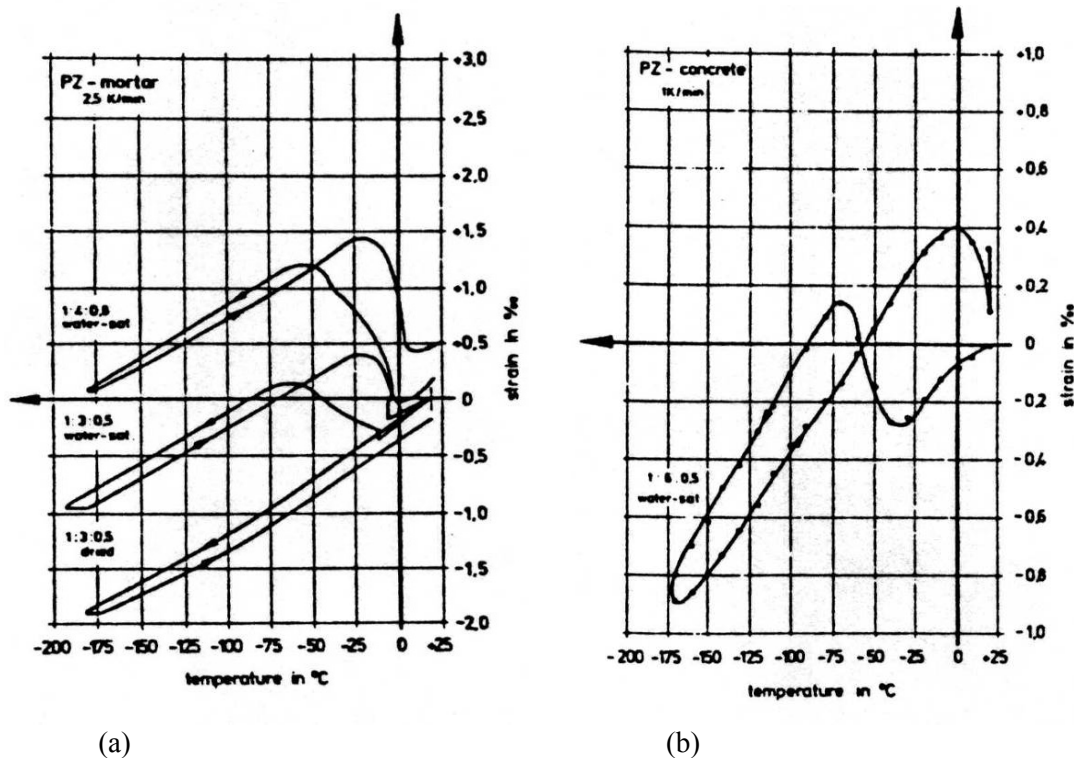


Figure 4.18: Temperature induced strains in mortar at various moisture (a) and water saturated concrete (b) [13]

The thermal coefficient of expansion, i.e., the slope of the curves in Fig. 4.18, increases from a minimum at -4°C up to a maximum at -15°C . In general, the thermal coefficient of expansion, neglecting the expansion due to freezing, is at low temperatures reduced to about $5\text{-}6 \cdot 10^{-6}/^{\circ}\text{C}$ from about $10\text{-}12 \cdot 10^{-6}/^{\circ}\text{C}$ (same as for steel, see Ch. 4.3.3) at ambient temperature.

The thermal coefficient of expansion, α , for concrete versus temperature is shown in Fig. 4.22.

The influence of different material- and environmental parameters on the ice formation is identified by freeze calorimetric experiments by De Fontenay and Sellevold [14], Sellevold and Bager [15], and Bager and Sellevold [16]. These results are shown in Fig. 4.19 to 4.21.

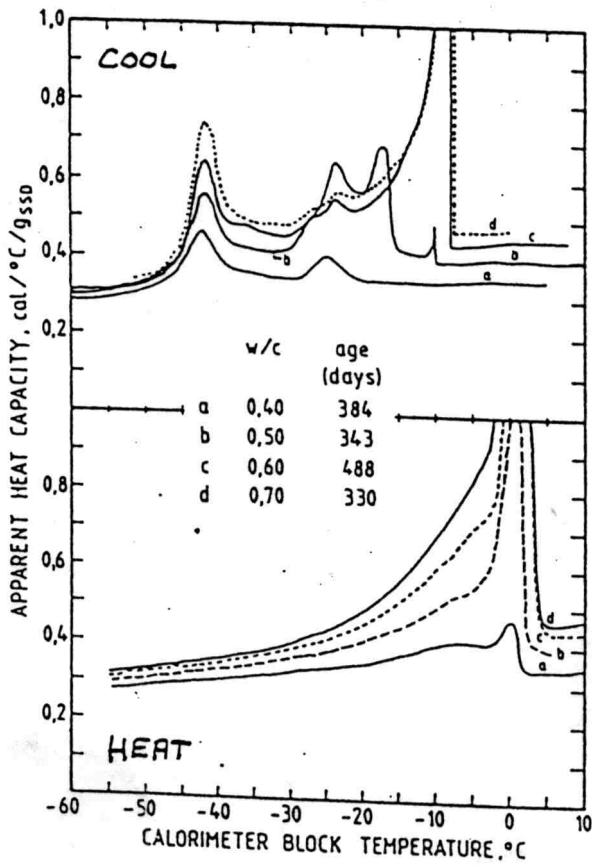


Figure 4.19: Ice formation in water saturated cement paste with different w/c-ratio. The area below the top of the curves is proportional with the amount of ice [14]

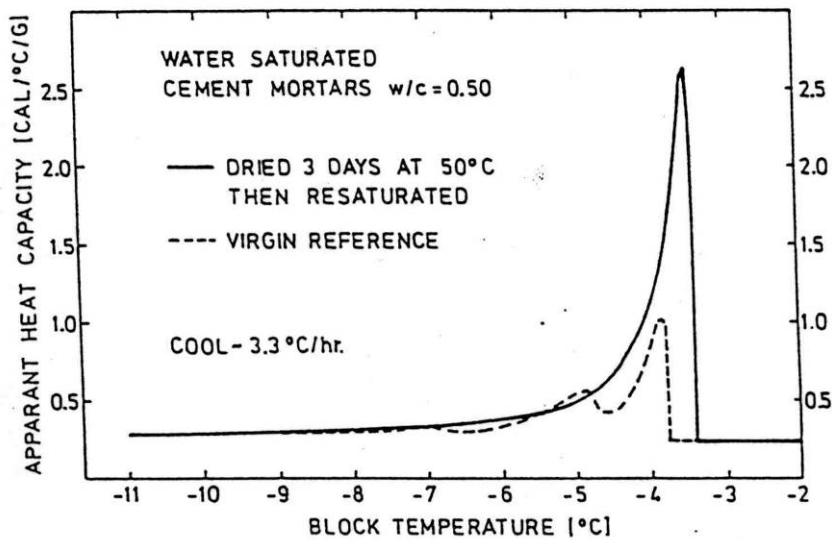


Figure 4.20: Ice formation in water saturated mortar before and after drying/saturation [15]

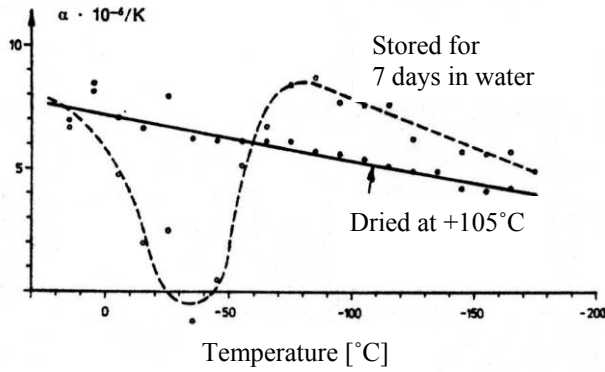


Figure 4.22: Thermal coefficient, α , of concrete versus temperature [17]

Fig 4.23 shows the thermal strain in water saturated cylinders during two thermal cycles. In the specimens subjected to an external load the micro crack development due to freezing of water is suppressed in the direction perpendicular to the load and, consequently, no expansion in the direction of the load is observed for temperatures from -20°C to -50°C [18].

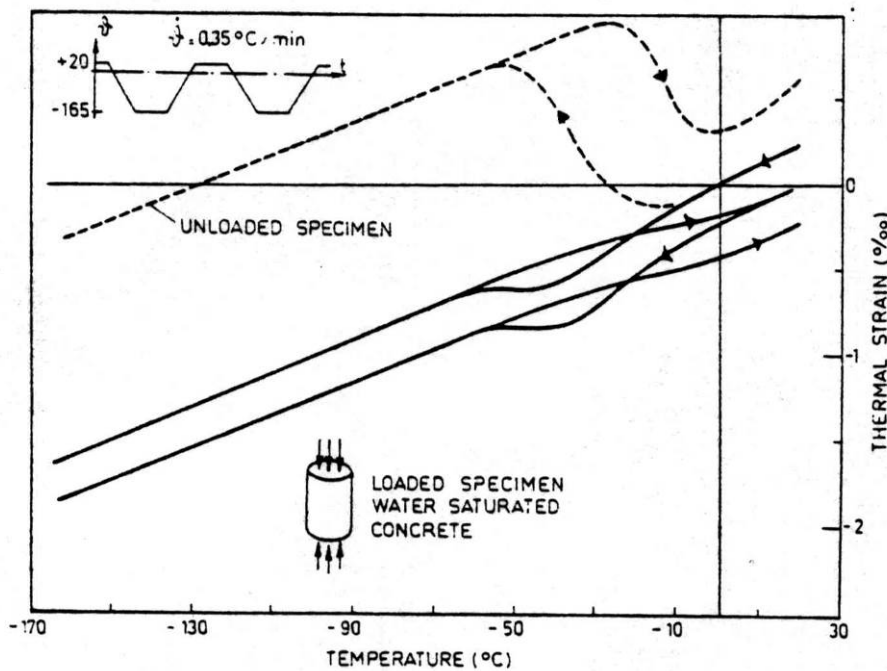


Figure 4.23: Thermal strains (%) in loaded and unloaded specimens versus temperature [18]

4.2.10 Thermal conductivity

According to tests referred by Wischers and Dahms [1] the thermal conductivity, λ , increases with reduced temperature as shown in Fig. 4.24. In both water saturated and moist cured specimens of normal density concrete the increase from $+20^{\circ}\text{C}$ to -160°C , was about 40%. A high moisture content increases the conductivity. In lightweight aggregate concrete the increase in conductivity with reduced temperature was almost negligible.

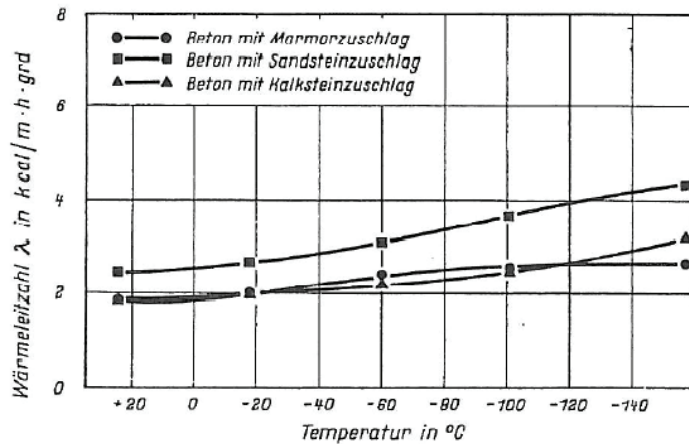


Figure 4.24: Influence of reduced temperature on the thermal conductivity, λ , of water stored concrete [1]. Filled circles, triangles and squares represent concrete with marmor, limestone and sandstone aggregate, respectively.

4.3 Steel properties at low temperatures

4.3.1 Introduction

The temperature has an influence on the mechanical properties for all types of steel. As for concrete the temperature level, the heating or cooling rate and the load history are of importance. The response to both low and high temperatures of different types of steel will vary depending on the production techniques used.

The structure of steel depends on the carbon content and on the cooling procedure from mass steel to solid steel bar at ambient temperature. The properties do also depend on whether the steel has been cold-worked or hot-rolled. If steel is reheated the properties will change.

At reduced temperature the failure mode of carbon steel changes from ductile to brittle. The temperature, at which this transition occurs, depends on several factors including carbon content, size of crystals, amount and presence of micro cracks and notches. The specimen size and the loading rate do also have an influence on the measured behaviour. For deformed bars hot spots may occur, which may be disadvantageous especially at low temperatures.

4.3.2 Stress-strain curves

Stress-strain curves for hot-rolled reinforcing steel at low temperatures are presented in Fig. 4.25. It is seen that the yield strength increases with decreasing temperatures. At the same time there is a tendency of reduced ductility. The size of the reduction may, however, vary significantly due to differences in the chemical composition of steel from different countries. Although the ultimate elongation is reduced, the ductility is considered to be sufficient. It is sufficient as long as the elongation after yielding exceeds the limit 4%, which is taken as an acceptable limit in the design against seismic loads.

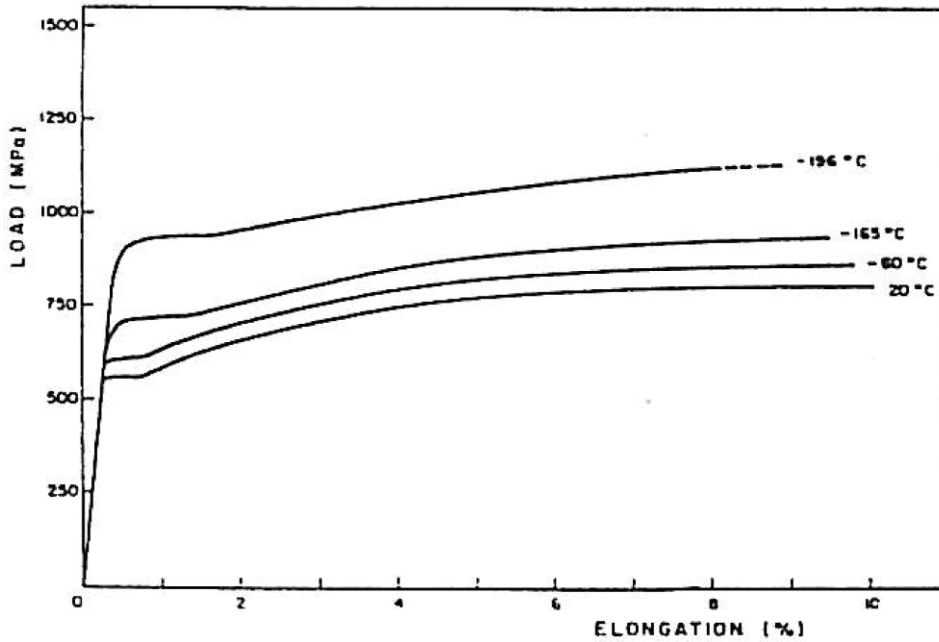


Figure 4.25: Stress-strain curves at low temperatures for hot-rolled reinforcement [19]

The stress-strain curves for cold-drawn prestressing wires are shown in Fig. 4.26. Again an increase in yield and ultimate strengths is observed at lower temperatures. The increase is, however, not as pronounced as for hot-rolled steels.

The ultimate elongation at low temperatures varies. In the investigation presented in Fig. 4.26, the elongation increases slightly when the temperature is reduced from +20°C to -165°C. Other results show, on the other hand, a significant decrease in the ultimate elongation.

Although, the ultimate elongation is often found to decrease, prestressing steels are normally considered to be well suited for low temperatures.

As for reinforcing steels, the modulus of elasticity of prestressing steels is not significantly influenced by low temperatures. When the temperature is reduced from +20°C to cryogenic conditions, the modulus of elasticity increases about 6-10% [8].

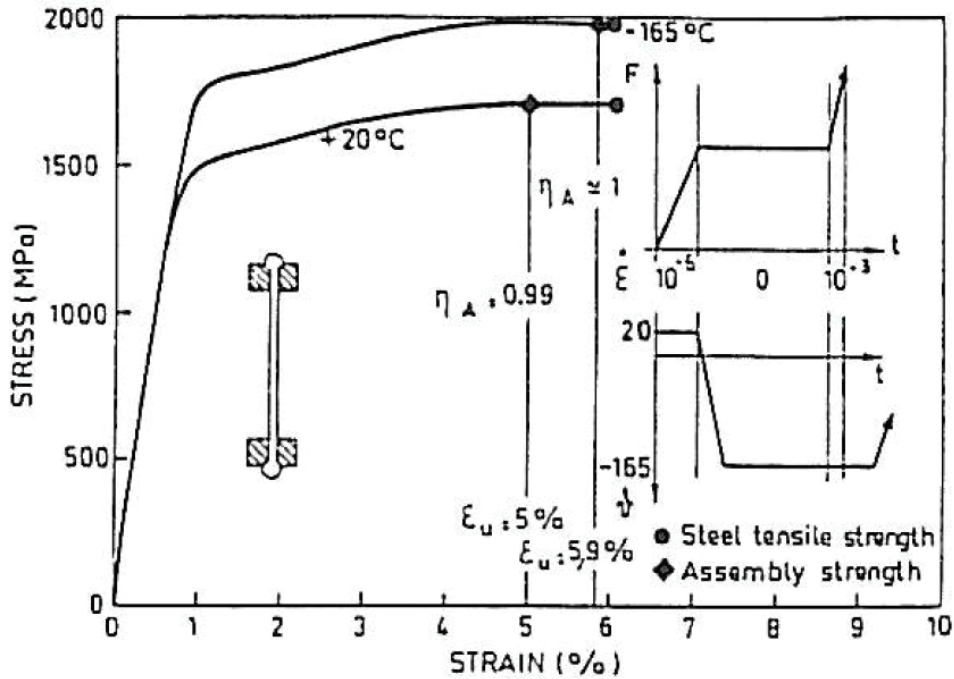


Figure 4.26: Stress-strain curves for cold-drawn prestressing wire at +20°C and -165°C [21]

4.3.3 Fracture toughness

The fracture toughness of steel may be determined by the Charpy pendulum impact test. In such tests a substantial drop in fracture energy is observed for hot-rolled and cold-worked steels already at temperatures in the range -20°C to -40°C [20]. The reduction in fracture energy is less pronounced for steel alloys containing nickel.

It is, however, questioned whether the fracture energy determined on notched specimens subjected to impact loads is representative of the toughness under service conditions. Impact tests on un-notched reinforcing bars, for instance, demonstrated ductile deformations even at -120°C.

The influence of temperature on the fracture toughness of hot-rolled steel determined in stable tests on three different types of notched specimens is shown in Fig. 4.27. The reduction in fracture toughness from +20°C to -196°C is about 50%.

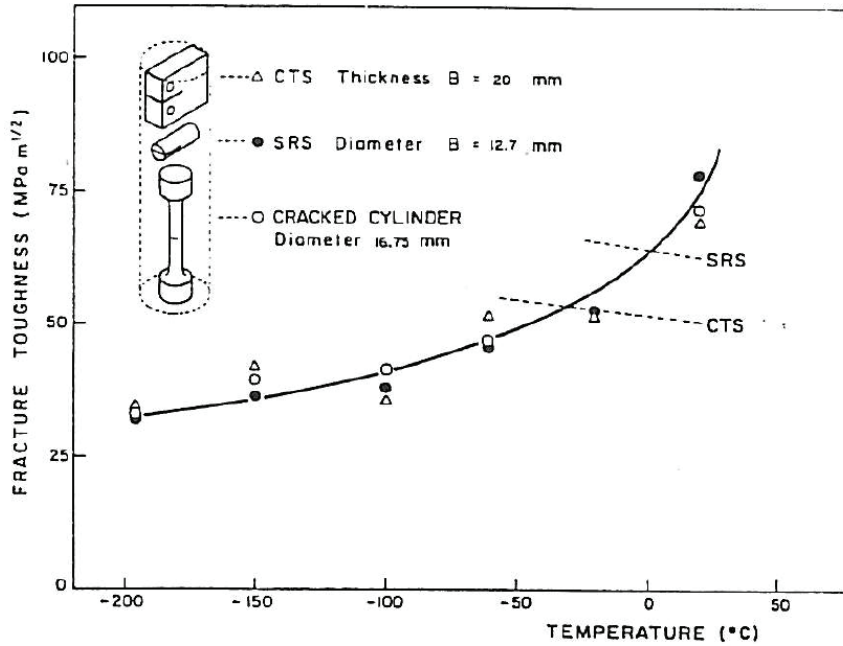


Figure 4.27: Influence of temperature on the fracture toughness of hot-rolled steel determined in stable tests on notched specimens [19]

4.3.4 The coefficient of thermal expansion at low temperature

For most types of steel the coefficient of thermal expansion, α , is considered to be constant in the temperature range -50°C to $+20^{\circ}\text{C}$. The α -value varies in the range $10\text{-}12 \cdot 10^{-6}/^{\circ}\text{C}$, depending on the steel quality. For reinforcing steels no change of α -value was found when the temperature was reduced from $+20^{\circ}\text{C}$ to -165°C , while for prestressing steel it was found to decrease from $10.5 \cdot 10^{-6}/^{\circ}\text{C}$ to $7.6 \cdot 10^{-6}/^{\circ}\text{C}$ at -165°C .

The α -value of concrete is reduced at low temperatures, see Ch. 4.2.9. The reduction corresponds approximately to the reduction for prestressing steel. Since the α -value is not reduced for the reinforcing steel, the contraction of the reinforcement will be larger than the contraction of concrete at cryogenic temperatures. This will cause tensile forces in the reinforcement and compressive forces in concrete. In the design of structures subjected to cryogenic temperatures it is, therefore, necessary to consider the influence of differences in α -values.

4.4 Constructional elements at low temperatures

Several tests with reinforced and prestressed concrete beams at low temperatures has been carried out to look into moment capacity, shear capacity and bonding- and anchor capacity.

4.4.1 Moment capacity

Fig. 4.28 shows a test rig for bending of reinforced concrete beams. Amount of reinforcement and temperature varied. Fig. 4.29 shows how moment of rupture for normal-reinforced beams and over-reinforced beams develops as function of temperature.

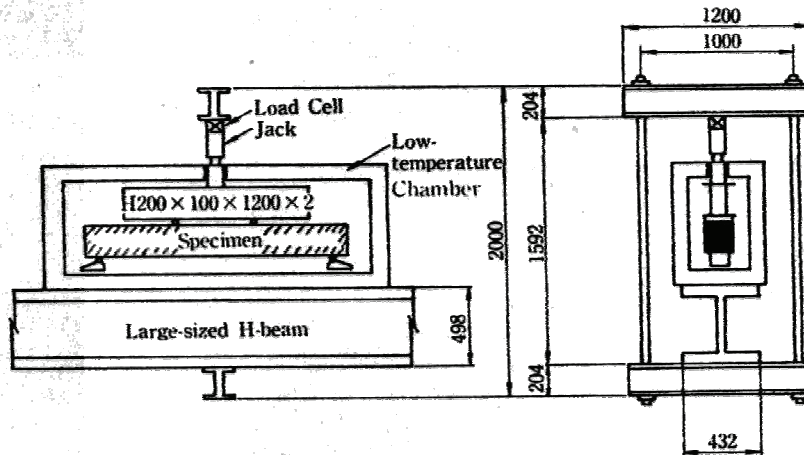


Figure 4.28: Test rig for concrete beam at low temperatures [22]

Fig. 4.29 is showing that by lowered temperature the moment of rupture increases considerably.

When it comes to both beams the increase is about 100% when the temperature is lowered from +20°C to -150°C

At the same time the increase of the yield stress of the reinforcement is about 75%, while the increase of the compressive strength of the concrete from +20°C to -105°C is 142% (from 38.3 to 92.6 MPa). The compressive strength at -150°C was not given [22].

When using standard procedures considering the increase in compressive strength for concrete and the yield stress of the reinforcement to estimate the moment of rupture the result is in accordance also at low temperatures.

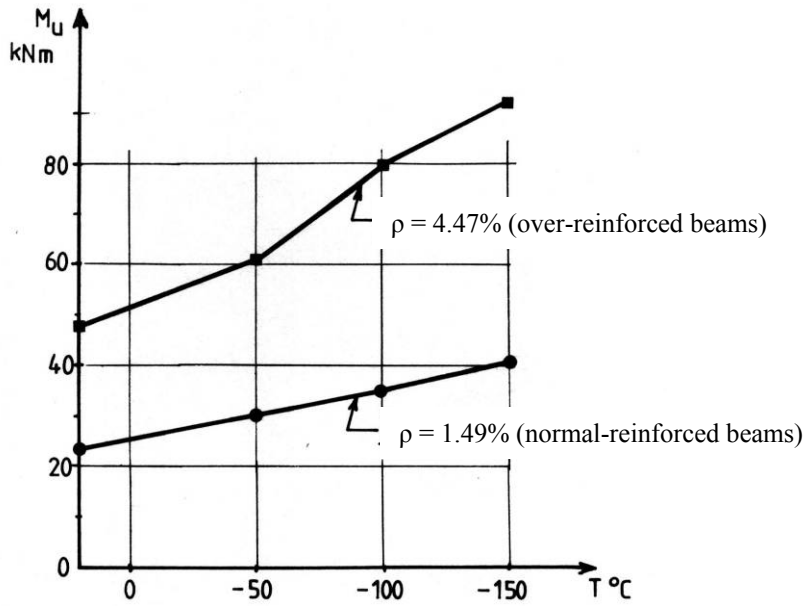


Figure 4.29: Fracture moment versus temperature and amount of reinforcement for water stored beams [22]

Okada and Iguro's [23] experiments on prestressed concrete beams also showed an increase of ultimate strain at the pressure edge at lowered temperature.

Fig. 4.30 shows the results from experiments with prestressed concrete beams. Two similar beams were tested at +20°C and -70°C.

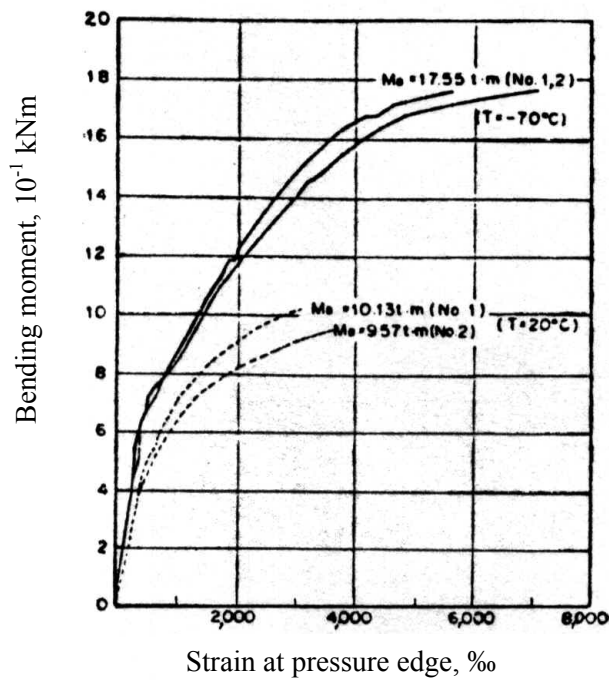


Figure 4.30: Strain at pressure edge of a prestressed concrete beam versus bending moment and temperature [23]

4.4.2 Shear capacity

According to shear capacity of reinforced concrete beams [24] tests have been carried out as showed in Fig. 4.31. The beams are continuous across two similar spans.

The following clamping conditions are used at the end supports: 1) Revolving and flexible in the longitudinal direction, 2) fixed and flexible in the longitudinal direction and 3) fixed and strapped against longitudinal change.

The beams were tested with standard procedures with monotonous load increase up to shear fracture at room temperature.

The beam which was to be cooled down was first loaded to a certain “application load”. Then the upper side of the beam was sprayed with liquid nitrogen (see Fig. 4.31), while the load was held constant. The cool down continued until it was a stable temperature gradient over the beams height (ca +20°C to - 196°C). Then the load was increased to fracture.

The purpose of this procedure was to simulate a load case by liquefied gas flowing towards a constructional element which is loaded and normally not exposed for lower temperature, ergo an accident load. As a result of this the experiments are not ideal to find shear capacity as a function of temperature. However the results are interesting.

FIG. 1

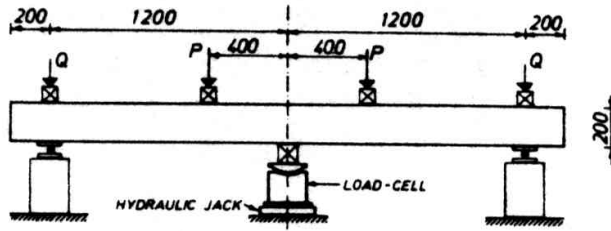


FIG. 2

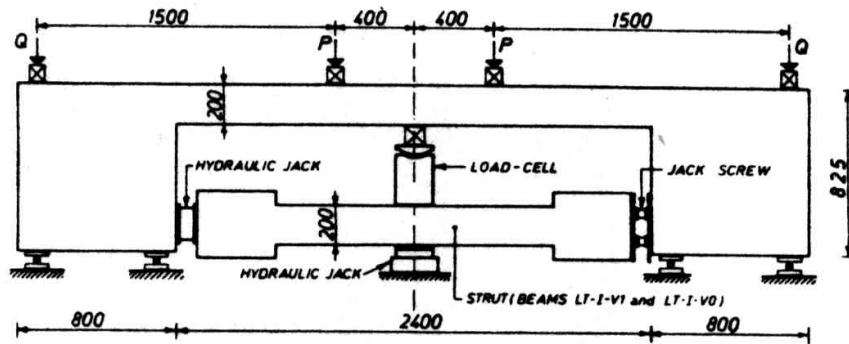


FIG. 3

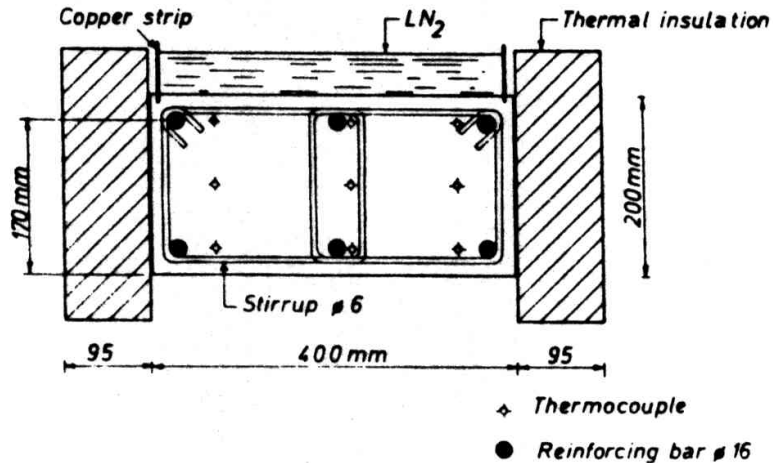


Figure 4.31: Test rig for concrete beams at low temperature [24]

For beams that have revolving end support and are flexible in the longitudinal direction, an increase in fracture load from 30-60% (related to a temperature at 20°C) was found depending on whether the beam had shear reinforcement or not.

The beams that had fixed end support and were flexible in the longitudinal direction also showed an increase in fracture load of about 60%. The beams that had fixed end support and were strapped against longitudinal change, so that the beam applied a tensile force, exhibited a reduction in fracture load of about 13%.

These experiments show both that the shear capacity increases with lowered temperature, but also that the capacity at temperature load like this is considerably affected by the support conditions.

However, it is first at complete restraint the shear capacity is reduced compared with +20°C.

The effect of restraint in the longitudinal direction is known from analogous experiments with fire load on concrete structures where the result of the expansion is an eccentric axial pressure and an appurtenant increase in shear capacity.

4.4.3 Bonding – and anchor capacity

According to the results showed in Ch. 4.2, there is reason to believe that the bonding capacity at anchoring of reinforcement in concrete also increases at lowered temperatures.

In Fig. 4.32 we can see that the anchor capacity (fracture) is doubled from +20°C to -160°C for an extension (bonding) experiment.

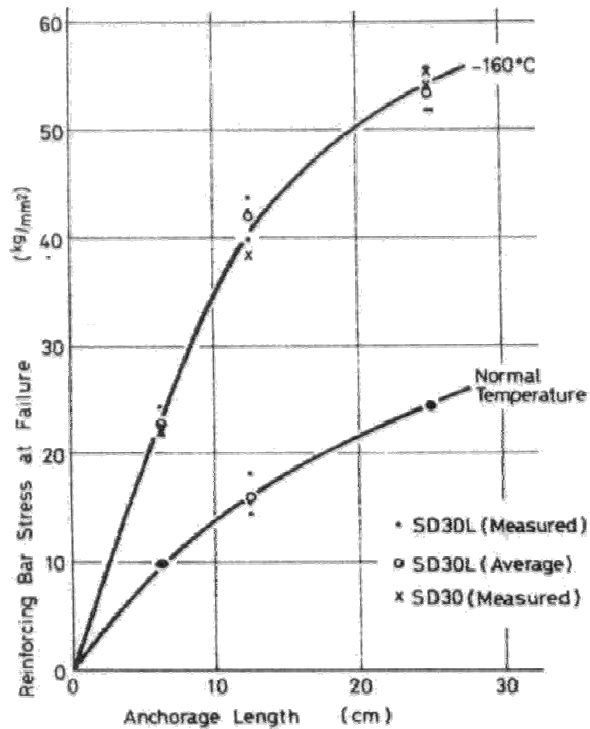


Figure 4.32: Reinforcing bar stress at failure versus anchorage length and temperature [25]

4.5 Concluding remarks due to low temperatures

4.5.1 Concrete properties at low temperatures

The strength of dry concrete is nearly unaffected by reduced temperatures. In moist concrete the strength is significantly increased, by a factor of three when the temperature is reduced from +20 °C to -100°C. This is due to the freezing of water in the pores and voids. The major problem with respect to concrete service under low temperature is the deteriorating effect of temperature cycles, especially if the concrete is water saturated. In storage tanks for LNG this problem may be avoided or at least controlled. Utilization of high strength concrete that has increased resistance towards freezing and thawing, may give beneficial results. A slow freezing rate is also advantageous.

4.5.2 Steel properties at low temperature

At low temperatures reinforcing steel becomes more brittle and the ultimate elongation is reduced. Nevertheless, the ductility is considered to be sufficient and prestressing steels are normally regarded to be well suited for low temperatures. The coefficient of thermal expansion is a little bigger than for concrete ($\Delta\alpha \approx 4 \cdot 10^{-6}/^{\circ}\text{C}$), which should be accounted for in calculations of tensions when cool-down of a reinforced concrete structure is relevant.

4.5.3 Construction elements at low temperature

Results are showing good functionality at cryogenic temperature for both reinforced and prestressed beams. However, it is important to take into consideration, by constructive design, the effect of temperature to reduce restraint forces that may occur.

Capacity

When the temperature is decreasing below 0°C , flexible structural elements of reinforced and prestressed concrete are normally showing a considerable increase of capacity regarding both axial-, moment- and shear force. The capacity of both axial- and moment force can be estimated with good accordance using standard procedures when the increased strength and possible reduced ultimate strain is taken into account. While the shear force capacity for flexible structural elements also increases, it may not be to the same extent as the increase of the tensile strength of the materials.

The coefficient of thermal expansion and mutual restraint

- The coefficient of thermal expansion (with normal range $10 - 12 \cdot 10^{-6}/^{\circ}\text{C}$) for the reinforcement seems to be rather independent of temperature. The concrete, which often has a lower coefficient compared with steel, normally get a certain reduction of the coefficient with lowered temperature. Concrete with a high degree of water content also get a considerable expansion caused by ice formation, especially at temperatures from -20 to -70°C .
- In most cases the expected pre-tensioning effect of internal restraint caused by a higher coefficient of thermal expansion for the reinforcement compared with concrete at low temperatures, may be favourable since it normally will reduce the development of tension cracks.
- The main effect of restraint stresses caused by temperature differences between various constructional elements is that this may cause development of cracks during cool-down. In this connection observations of the expansion of concrete caused by ice formation at temperatures from -20 to -70°C seems to disappear when the concrete has a pressure load.
- Restraint stresses caused by hindered temperature shortening may lead to reduced fracture capacity. This is especially determining for the shear capacity due to not shear reinforced structures. The resulting requirement due to crack dispersion at cryogenic temperatures is increased amount of minimum reinforcement.

Deterioration due to cyclic temperature variations

- After cryogenic temperature cycles, tests are showing that the concrete obtain reduced stiffness and strength at climatic temperatures. In addition to the minimum temperature and number of cycles the damage is also especially dependent on the concretes water saturation. Accordingly increased water content causes increased strength in cold condition, but also increased damage after warm-up.
- It is likely that the same parameters which are increasing the frost resistance of the concrete at climatic conditions also will reduce the damage at cryogenic temperature cycles. Increased frost resistance is achieved by reduction of w/c ratio (increased strength) and use of air entraining admixtures. Moist curing over a relative long time period, reduction in water content before freezing and reduced speed of cool-down are also assumed to reduce the frost damage.
- The extent of the observed strength reduction is dependent of how many cryogenic temperature cycles the structure will be exposed to.

5 Effect of water pressure on concrete structures

In the SINTEF report STF65 A90005 [47] water absorption, water penetration and permeability of concrete are briefly reviewed. The knowledge of the effect of water and water pressure on concrete structures loaded by static and dynamic loads is also summarized. This report [47] is a state of the art of the effect of water pressure on concrete structures, and is not reviewed in this preliminary study. However, the content in the SINTEF report [47] is considered to be relevant if the primary objective in further research can be related to concrete structures exposed to water pressure.

The main contents in SINTEF Report STF65 A90005 [47] are:

- Effect of water and water pressure:
 - Water absorption, water penetration and permeability (herein also influence of sea water)
 - Effect of pore pressure
 - Deformation properties of submerged concrete
 - Concrete strength under hydrostatic pressure
 - Hydrostatic loaded beams
- Fatigue strength of concrete in water:
 - Normal density concrete
 - Light weight aggregate concrete
 - Concrete strength under hydrostatic pressure

6 Conclusions and further research

To achieve an impervious concrete structure, it is assumed that the main challenge is related to prevention of crack formation. This can be achieved through a combination of proper structural design and materials technology. If the structure is exposed to cryogenic temperatures, special considerations must be taken to prevent development of cracks, especially if the structure also is supposed to be the impervious barrier without supplement of any gas and liquid tight membrane. A considerable number of factors that somehow may affect the tightness of concrete structures (e.g. temperature, degree of saturation, crack width, etc.) are summarized in this report.

In further work regarding tightness of concrete structures it is necessary to make more specific:

- Primary objective due to functionality, acceptance criterion with respect to tightness, etc.
- Type of gas and/or liquid (Water, Propane, Nitrogen, LNG, etc) that should be focused on, herein whether the tightness has to resist diffusion (i.e. concentration gradients) and/or permeation (i.e. pressure gradients).
- Type of structure, e.g. volume, height, width, etc.

Most likely it will be important to see this project in relation with the material approach in COIN P1 (advanced cementing materials) and COIN P2 (improved construction technology), as shown below.

The following primary objectives should be considered to achieve requested tightness:

1. Concrete (mixture proportions) with sufficiently low diffusivity and permeability due to actual gas and/or liquid exposure → (COIN P1)
2. Prevent cracks in the curing process caused by shrinkage and early thermal contraction (external- and internal restraint) → (COIN P2)
3. Maintain the tightness (prevent cracks) during the operating time of the structure → **COIN P3**

Based on point 3 above the following should be considered in further work:

- 3.1 Investigate tightness criterion based on actual gas/liquid, mixture proportions and acceptance criterion:
 - Sufficient depth of the compressive zone.
 - Sufficient depth of the overall construction (cross-section of wall, roof, etc.).
 - Sufficient amount and performance of reinforcement and prestressing steel.
 - Sufficient limitation of cracks due to crack widths and crack depths.
- 3.2 Development of models to predict diffusivity and permeability from geometrical data including cracks (point 3.1 above), mixture proportions (point 1. above) and exposure conditions (type of gas or liquid, pressure gradients, concentration gradients, temperature, etc.). Review of existing calculation models should be a part of this work, together with supplementary experiments.

- 3.3 Development of constructional design in order to prevent cracks caused by static and dynamic loads (shear cracks and tension bending cracks), herein:
- Design that prevent mutual restraint and appurtenant possible tensile forces between different constructional elements caused by external load and internal forces from prestressing wires, etc., for a statically undetermined structure.
 - Details such as construction joints (flexible joints, sliding plates, etc.), formwork ties and inserts may have to be treated with respect to both tightness and functionality to satisfy the condition in the calculation model.
- 3.4 Development of design to prevent cracks caused by temperature gradients in the structure and restraint between different constructional elements:
- Design as listed in point 3.3.
 - Insulation
 - Functional description for technical installations to maintain sufficient uniform temperature distribution in the structure (cooling tubes, etc.).
- 3.5 Development of methods to re-establish sufficient tightness:
- Method to re-establish sufficient tightness concerning possible damages due to bad concreting, such as honeycombs and badly compacted concrete.
 - Method to re-establish sufficient tightness hampered by possibly occurring dead- or living cracks.
- 3.6 For structures exposed to cryogenic temperatures (e.g. LNG tanks) some additional effects may be crucial for the structures tightness and should therefore be investigated:
- Design to prevent mutual restraint also in case of shutdown.
 - Deterioration in case of shut down (see Ch. 4.2.6)
 - Possible negative effects of the difference between concrete and reinforcement due to the coefficient of thermal expansion at low temperatures (see Ch. 4.2.9, 4.3.4 and 4.5.2).
 - Positive and negative influence of temperature depression and appurtenant ice formation (see Ch.3.2, 4.2, 4.3 and 4.4).
- 3.7 Possible superimpose of e.g. diffusion (result of concentration gradients) on other transport phenomena such as:
- penetration caused by pressure gradients
 - convection (result of temperature gradients)
 - migration
 - capillary suction (pumping effect caused by cycles of wetting and drying)

References

- [1] Wischers, G. and Dahms, I.: *"Das Verhalten des Betons bei sehr niedrigen Temperaturen"*, Beton-Verlag GmbH, 1970.
- [2] Berner, D., Gerwick, B.C. and Polivka, M.: *"Static and Cyclic Behaviour of Structural Lightweight Concrete at Cryogenic Temperatures"*, in *Temperature Effects on Concrete*, ASTM Sp. Tech. Publ. No. 858, pp.21-37 (Philadelphia, Pa, 1983).
- [3] Miura, T.: *"The properties of Concrete at Very Low Temperatures"*, *Materials and Structures*, Vol. 22, No. 130, 1989, pp. 243-254
- [4] Goto, Y. and Miura, T.: *"Experimental Studies on Properties of Concrete Cooled to about Minus 160 °C"*, *Technical Reports, Tohoku University*, Vol. 44, No. 2, 1979, pp. 357-385.
- [5] Rostásy, F.S. and Wiedemann, G.: *"Stress-Strain-Behaviour of Concrete at Extremely Low Temperature"*, *Cement and Concrete Research*, Vol. 10, 1980, pp. 565-572.
- [6] Marshall, A.L.: *"Marine Concrete"*, Blackie and Son Ltd, Glasgow, 1990
- [7] Yamane, S., Kasami, H., Okuno, T.: *"Properties of Concrete at Very Low Temperatures"*, Douglas McHenry International Symposium on Concrete and Concrete Structures, ACI SP-55, 1978, pp. 207-221.
- [8] Turner, F.H.: *"Concrete and Cryogenics"*, Viewpoint, Cement and Concrete Association, 1979
- [9] Hoff, A.: *"Betongens bruddtøyning ved lave temperaturer"*, SINTEF rapport STF65 A82059, 1982.
- [10] Rostásy, F.S. and Wiedemann, G.: *"Strength and Deformability of Concrete after Low Temperature Cycles"*, Second Int. Conf. on Cryogenic Concrete, Amsterdam, okt. 1983.
- [11] Körmeling, H.A.: *"The Rate Theory and the Impact Tensile Behaviour of Plain Concrete"*, In *"Fracture Toughness and Fracture Energy of Concrete"*, Ed. F. Wittmann, Elsevier, Amsterdam, 1986, pp. 467-477.
- [12] Okada, T. and Iguro, M.: *"Bending Behaviour of Prestressed Concrete Beams under Low Temperature"*, *Journal of Japan Prestressed Concrete Association*, Vol. 120, No. 5, 1978.
- [13] Rostásy, F.S., Schneider, V. og Wiedemann, G.: *"Behaviour of Mortar and Concrete at Extremely Low Temperatures"*. *Cement and Concrete Research*, Vol. 9, 1979.
- [14] De Fontenay, C. and Sellevold, E.J.: *"Ice Formation in Hardened Cement Paste I"*, ASTM, STP 691, Ottawa, 1980.

- [15] Sellevold, E.J. and Bager, D.H.: *“Implications of Calorimetric Ice Formation Results”*, Proceedings of Nordic Seminar, Køge, 1984, Publication No- 22, Danish Concrete Association.
- [16] Bager, D.H. and Sellevold, E.J.
“Ice Formation in Hardened Cement Paste II”,
ASTM, STP 691, Ottawa, 1980.
- [17] Kordina, K. and Neisecke, J.
“Die Ermittlung der Gebrauchseigenschaften von Beton und Spannstahl bei extrem tiefen Temperaturen”, Betonwerk + Fertigteil-Technik, Heft 4/1978.
- [18] Planas, J., Corres, H., Chueca, R., Elices, M., Sanchez-Galvez, V.
“Influence of Load on Thermal Deformation of Concrete during cooling down”
Second Int. Conf. on Cryogenic Concrete, Amsterdam, okt. 1983.
- [19] Valiente, A., Mestre, A. et al: *“Fracture at Low Temperatures of Steels for Concrete Reinforcement”* Second Int. Conf. on Cryogenic Concrete, Amsterdam okt. 1983.
- [20] Adams, M.A.J.: *“Selection of Steels for Reinforcement and Prestressing of Concrete at Cryogenic Temperatures”* Second Int. Conf. on Cryogenic Concrete, Amsterdam, okt. 1983.
- [21] Corres, H., Planas, J. et al: *“Behaviour of Tendon-Anchorage Assemblies under Cryogenic Conditions”*, Second Int. Conf. on Cryogenic Concrete, Amsterdam, okt. 1983.
- [22] Goto, Y. and Miura, T.: *“Bending Properties of Reinforced Concrete Beams and Lapped Splice Strengths of Reinforcing Bars at Very Low Temperatures”*,
Technology Reports, Tohoku Univ., Vol. 45, No. 1, 1980.
- [23] Okada, T. and Iguro, M.: *“Bending Behaviour of Prestressed Concrete Beams under Low Temperature”*, Publikasjon ukjent.
- [24] Taerve, L. and de Saint Moulin, I.: *“Loading Tests on Reinforced Concrete Beams at Low Temperature”*, Second Int. Conf. on Cryogenic Concrete, Amsterdam, okt. 1983.
- [25] Goto, Y. and Miura, T.: *“Experimental Studies on Properties of Concrete Cooled to About Minus 160 °C”*, Technology Reports, Tahoku Univ., Vol. 44, No. 2, 1979.
- [26] A.M. Thyler: *“A review of data on spreading and vaporisation of cryogenic liquid spills”*
Journal of Hazardous Materials A99 (2003) 31-40
- [27] Hans-Wolf Reinhardt, Martin Jooss: *“Permeability and self-healing of cracked concrete as a function of temperature and crack width”*
Cement and Concrete Research 33 (2003) 981-985
- [28] Martin Jooss, Hans W. Reinhardt.
“Permeability and diffusivity of concrete as function of temperature”
Cement and Concrete Research 32 (2002) 1497-1504

- [29] Marta Choinsk, Abdelhafid Khelidj, George Chatzigeorgiou, Gilles Pijaudier-Cabot.
“Effects and interactions of temperature and stress-level related damage on permeability of concrete”
Cement and Concrete Research 37 (2007) 79-88
- [30] Abdalla M. Odeh, Wa’il Abu-El-Sha’r, Rami Al-Ruzouq.
“Gas transport through concrete slabs”
Building and Environment 41 (2006) 492-500
- [31] Ludovic Jason, Gilles Pijaudier-Cabot, Shahrokh Ghavamian, Antonio Huerta.
“Hydraulic behaviour of a representative structural volume for containment buildings”
Nuclear Engineering and Design 237 (2007) 1259-1274
- [32] J. P. Monlouis-Bonnaire, J. Verdier, B. Perrin.
“Prediction of the relative permeability to gas flow of cement-based materials”
Cement and Concrete Research 34 (2004) 737-744
- [33] Ha-Won Song, Seung-Jun Kwon, Keun-Joo Byun, Chan-Kyu Park.
“Predicting carbonation in early-aged cracked concrete.”
Cement and Concrete Research 36 (2006) 979-989.
- [34] S. A. Meier, M.A. Peter, M. Böhm.
“A two-scale modeling approach to reaction-diffusion processes in porous materials.”
Computational Materials Science 39 (2007) 29-34.
- [35] L. Marsavina, K. Audenaert, G. De Schutter, N. Faur, D. Marsavina.
“Experimental and numerical determination of chloride penetration in cracked concrete.”
Construction and Building Materials xxx (2008) xxx-xxx (“article in press”).
- [36] A. Djerbi, S. Bonnet, A. Khelidj, V. Baroghel-bouny.
“Influence of traversing crack on chloride diffusion into concrete.”
Cement and Concrete Research xx (2008) xxx-xxx (“article in press”).
- [37] R. Ohba, A. Kouchi, T. Hara, V. Vieillard and D. Nedelka.
“Validation of heavy and light gas dispersion models for the safety analysis of LNG tank”
Journal of Loss Prevention in the Process Industries 17 (2004) 325-337
- [38] COSMAR: Part Project 1 (PP1):
“Investigation of Offshore Concrete Structures with Respect to Static Strength”
- [39] COSMAR: Part Project 2 (PP2):
“Investigation of Offshore Concrete Structures with Respect to Fatigue Strength”
- [40] COSMAR: Part Project 3 (PP3), report no. PP 3-4-4:
“Calculation of Leakage Rates of Uncracked and Cracked Concrete structures”
- [41] COSMAR: Part Project 3 (PP3), report no. PP 3-5-3:
“Tests for Determination of the Permeability of Uncracked Concrete”

- [42] COSMAR: Part Project 3 (PP3), report no. PP 3-5-4:
“Tests for Determination of the Permeability of Cracked Concrete”
- [43] COSMAR: Part Project 3 (PP3), report no. PP 3-6-1:
“Design Criteria for Marine Concrete LNG Structures”
- [44] COSMAR: Part Project 3 (PP3), report no. PP 3-6-4:
“Liquid Tightness of LNG Storage Tanks”
- [45] COSMAR: Part Project 3 (PP3), report no. PP 3-6-6:
“Design criteria for concrete LNG tanks in a marine environment”
- [46] COSMAR: Part Project 3 (PP3), report no. PP 3-3-3:
*“Properties of Flowable Normal-Weight Concrete B45 in a Temperature Range
from
 $T = +20^{\circ}\text{C}$ to $T = -190^{\circ}\text{C}$ ”*
- [47] L. Bjerkeli: *“Effect of water pressure on concrete structures”*, SINTEF report
STF65 A90005, 1990.
- [48] Powers, T.C.: *“The Physical Structure and Engineering Properties of Concrete”*,
PCA Res. Dept. Bull., 90 (1958).

SINTEF Building and Infrastructure is the third largest building research institute in Europe. Our objective is to promote environmentally friendly, cost-effective products and solutions within the built environment. SINTEF Building and Infrastructure is Norway's leading provider of research-based knowledge to the construction sector. Through our activity in research and development, we have established a unique platform for disseminating knowledge throughout a large part of the construction industry.

COIN – Concrete Innovation Center is a Center for Research based Innovation (CRI) initiated by the Research Council of Norway. The vision of COIN is creation of more attractive concrete buildings and constructions. The primary goal is to fulfill this vision by bringing the development a major leap forward by long-term research in close alliances with the industry regarding advanced materials, efficient construction techniques and new design concepts combined with more environmentally friendly material production.

